Potential impacts of the Monterey Accelerated Research System (MARS) cable on the seabed and benthic faunal assemblages 2020

L.A. Kuhnz, K. Buck, C. Lovera, S. Litvin, P.J. Whaling, J.P. Barry
Monterey Bay Aquarium Research Institute

DOI: 10.13140/RG.2.2.12907.57122

SUMMARY

This report summarizes efforts to assess the condition of the MARS cable and its potential effects on surficial sediments and biological communities, based on an initial biological assessment in 2004, Post-Lay Inspection and Burial Survey (PLIB) in 2007, and comprehensive surveys performed in 2008, 2010, 2015 and 2020. The most recent study was conducted 13 years after the cable was installed. Note that this report supersedes information included in prior impact survey reports (2008, 2010, 2015). The sampling program was designed to:

- Observe the condition of the cable and cable path along the 60 km cable route,
- Assess the potential impacts of the MARS cable on surficial geological conditions and benthic biological assemblages on a local scale (0–50 m from the cable) and at a regional scale (km), based on video transects and sediment samples.

We conclude that the MARS cable has had little detectable impact on seabed geomorphology, sediment qualities, or biological assemblages. Specific conclusions include:

- Over most of its length the cable remains buried, with some evidence of change since installation
  - The cable has remained buried along shallow portion of the cable route.
  - Sediment has filled the cable trench in deeper areas, which is now nearly imperceptible in most locations.
  - Along the rocky section where the cable was not buried, some minor spans in the cable are present due to small-scale bathymetric complexity. No major spans or suspensions were present.
  - Trawling occurred near the MARS node at least three times between 2009–2010, damaging two instruments and an auxiliary cable. We detected that an unburied 1350 m-long section of cable has moved 135 m to the SW, likely due to these, or subsequent trawling events.

- Minor differences in mean grain size were detected in relation to the MARS cable.

- The organic carbon content of sediments increased near the MARS cable at two depths, possibly due to natural variation, effects of the cable, or both.

- Local-scale variation in benthic megafaunal communities near (within 50–100 m) the MARS cable was minor or undetectable for the first three comprehensive surveys (2008, 2010, 2015). In 2020, the density of megafauna had increased at two of 10 stations and was significantly greater along the cable route than the undisturbed area just 50 m away. As in earlier surveys the cable was still exposed at both stations, with increasing numbers of attached anemones. The primary faunal change, however, was the large number of sea stars and sea cucumbers observed feeding on dead and dying midwater pyrosomes that had accumulated near the cable at a single station. Pyrosomes had not been observed previously along the cable route, and appeared to accumulate near the cable due to small-scale, near-bottom currents.

- In 2008, prior to energizing the cable, Longnose skates (*Beringraja rhina*) were significantly more abundant along minor suspensions of the cable (2–10 cm above the bottom, for intermittent short distances (1–3 m) over about 600 total linear m) along the rocky portion of the cable route near 300 m depth. *B. rhina* may have responded to mild electromagnetic fields generated by components of the cable. In 2010, 2015, and 2020 when the cable was powered, skate densities along the cable did not differ from an area 50 m away.

- The MARS cable has had little to no detectable effect on the regional-scale (i.e., km) distribution and density of macrofaunal and megafaunal assemblages.

- Faunal patterns compared before and after cable installation among three control stations and one cable station within each of three regions (Shelf: < 200 m, Neck: 200–500 m, Slope: > 500 m) indicated a very minor influence of the MARS cable installation on benthic biological patterns.

- Natural spatial and temporal variation in the density and distribution of benthic macrofauna and megafauna appears to be greater than the effects of the MARS cable.

Table of Contents

INTRODUCTION

The Monterey Accelerated Research System (MARS) is a 60 km-long undersea cable spanning from the Monterey Bay Aquarium Research Institute (MBARI) in Moss Landing, California to a science node at a depth of 891 m on the continental slope. The node is 45.5 km offshore, just outside of Monterey Bay, California (Fig. 1). The system provides power and high data bandwidth for science instruments connected to the node via thin auxiliary cables deployed on the seabed by remotely operated vehicles (ROVs). MARS is one of a now growing number of cabled ocean-observing systems that enable continuous, long-term science capabilities for ocean science with real-time communication, control, and data capture from offshore subsea sensor systems (Howe et al., 2019; Martin Taylor, 2008; Suyehiro et al., 2003; Trowbridge et al., 2019).

The main MARS cable was installed in March 2007 from the cable-laying ship *Global Sentinel.* The cable was installed beneath the seabed for most of its length. Horizontal directional drilling (HDD) was used to install a steel 13 cm diameter pipe conduit from above the shoreline to 19 m water depth offshore (Barry et al., 2007). From this point, the cable was plowed into the seabed sediment to a depth of one meter for most of its length, and jetted into the sediment near the science node at the MARS site (Figure 1). Complete burial was not possible in the rocky seabed (authigenic carbonate crusts and rocky outcrops) at depths of 116–453 m below the continental shelf break. The MARS science node was installed and powered briefly in February 2008, but failed due to a subsea connector. The failed parts were recovered, repaired, and reinstalled in November 2008. MARS has been fully operational since that time.

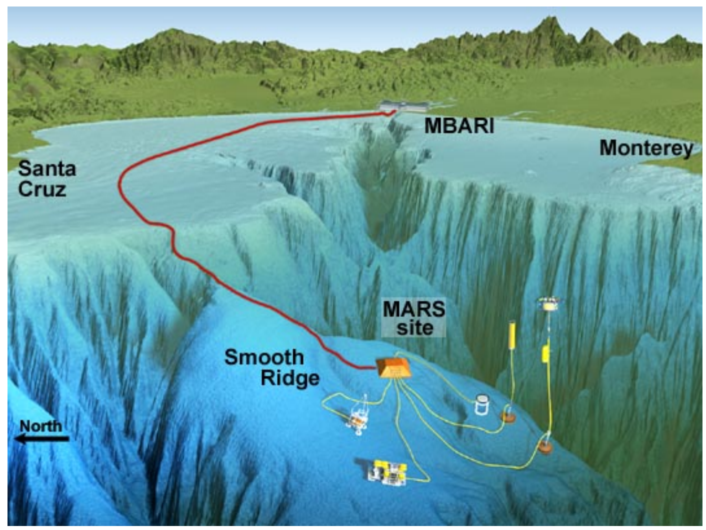

Figure 1. View of the MARS cable, node, and potential science instruments looking east over exaggerated bathymetry of Monterey Bay, Monterey Canyon, and the continental slope. The science node is indicated as "MARS site".

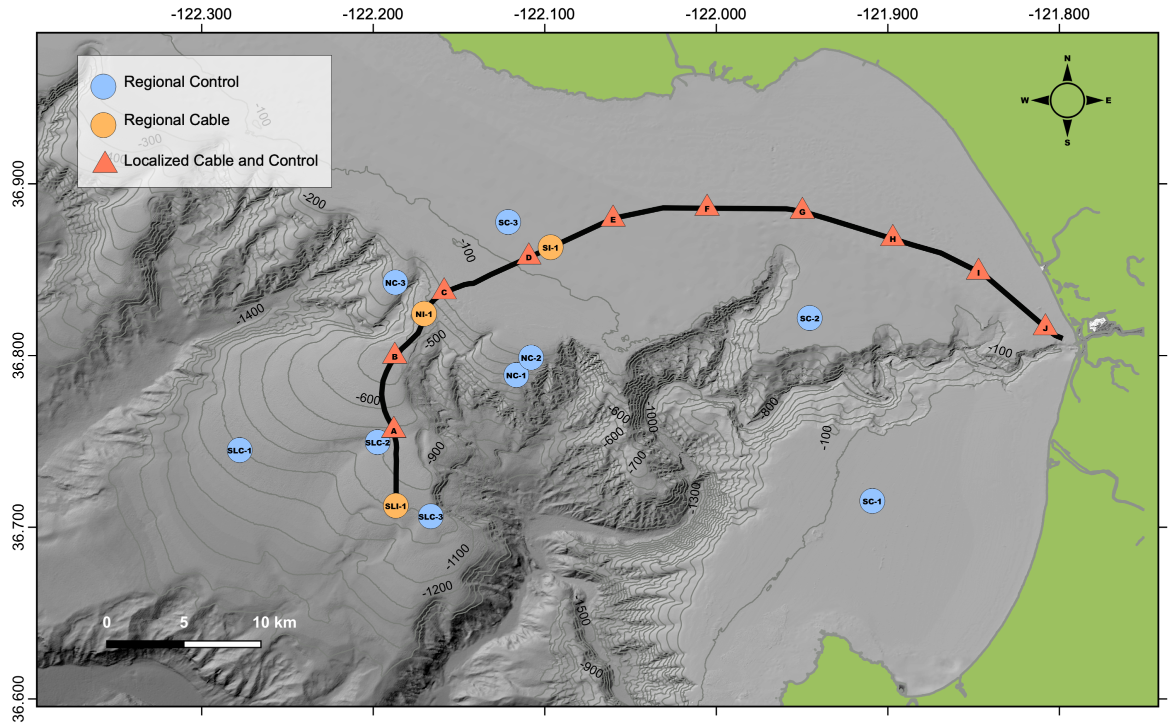

Figure 2. Map of Monterey Bay, the MARS 60 km cable route (black line) and environmental study stations. Colored circles represent regional stations for megafaunal and macrofaunal impact studies at Shelf, Neck, and Slope regions. Blue = control, light orange = cable. Lettered triangles (A−J) indicate transect stations for localized megafaunal studies on the cable route, paired with transects 50 m away from the cable. The MARS instrument node (station SLI-1) is on the seafloor at 891 m depth about 45.5 km from Moss Landing, in central California.

Prior to installation of the MARS cable a 2004 environmental impact report was produced to characterize seabed biological communities along the cable route, using initial video and macrofauna sampling. Data were also used as preparation for future environmental impact assessments (Fig. 2). This survey included characterization of megafaunal animals (epibenthic) and macrofaunal organisms (infaunal worms, crustaceans, etc., counted from sieved sediment samples) along the cable route. Subsequent to the MARS cable installation, a visual Post-Lay Inspection and Burial (PLIB) (Barry et al., 2007) ROV survey of the entire route was conducted (March 16–March 22, 2007 and June 7, 2007).

Following installation of the MARS cable, an initial environmental impact assessment was required within 18-months, along with subsequent assessments at 5-year intervals, including observations of the condition of the cable and potential effects on biological communities. In this report, we present all data from the 2004 pre-installation environmental impact assessment and post-installation surveys from 2008, 2010, 2015 and 2020.

METHODS

Cable and seabed condition

The initial position and condition of the cable was assessed along its route to the MARS node using MBARI's ROV *Ventana*. During the PLIB in 2007, the precise position and depth of the cable was determined along the buried portion of the cable route using an ROV-mounted cable sensing system (Teledyne TSS; flown 1–4 m above the seabed). The cable tracking system was not used in subsequent surveys (2008, 2010, 2015, 2020), and the condition of the cable was assessed with sonar and visual observations along most of the cable route. Burial of the cable in shallow, low visibility sections was confirmed by sonar and by crisscrossing the known route to look for evidence of the cable.

Near-bottom water clarity and fishing operations occasionally impaired or prevented ROV operations, particularly in shoreward cable sections. Very low or zero visibility conditions in shallow water prevented safe operation of the ROV. Stations exhibiting these conditions were generally checked at least twice per sampling season but surveying them was sometimes impossible. Commercial crab traps positioned along the shallow end of the cable route occasionally prevented the deployment of the ROV and disrupted cable surveys.

All observations of the seabed along the cable route and all sample collections were performed using MBARI's ROV *Ventana* supported by *R/Vs Point Lobos* and *Rachel Carson* and ROV *Doc Ricketts*, supported by the *R/V Western Flyer*. The main camera on each of the ROVs is an Ikegama high definition camera with a HA10Xt2 Fujinon lens, mounted on a 3-axis pan and tilt capable of +/- 45º of tilt. Two robotic manipulator arms were used on each ROV for sampling seabed sediments with push cores, which were stored in sample drawers. All dives were recorded and video of the entire route was annotated using MBARI's Video Information and Reference System (VARS) (Jacobsen Stout et al., 2020; Schlining and Stout, 2006). Non-quantitative surveys of portions of the cable route were recorded in an approximately 4 m–wide field of view. Observations included:

- burial status of the cable
- status of surficial damage to the seabed related to cable installation
- condition of the burial trench (i.e., cable exposed, partially or infilled with mud)
- cable condition, if exposed (lying on seabed or spanned between surficial geological objects)
- sessile megafauna present on the cable

Quantitative megafaunal video transects

Densities of megafaunal organisms were obtained from the analysis of quantitative video transects. For each video transect the ROV camera was tilted ~45 degrees from horizontal) to provide a perspective view of the seabed and zoomed so that the width of the image at the level of the lasers, as viewed in the center of the image, was just over 1 m. Each transect was run at ~0.1–0.2 ms^{-1} over a distance of 100 m. Paired parallel lasers (23 cm apart on *Ventana*, 29 cm apart on *Doc Ricketts*) provided a reference scale for estimating the spatial dimensions of the video image. Voucher specimens were collected as needed for additional taxonomic study.

Video transects were annotated using the VARS annotation system in a quantitative manner to provide estimates of the density (# 100 m^{-2}) of identifiable organisms (generally > 2 cm in size). Megafaunal organisms were identified to the lowest practical taxonomic level. Owing to the difficulty of identifying organisms based on video images, we were conservative in assigning taxonomic names. To avoid counting-bias due to field of view distortion, only those animals passing through the 1 m–wide swath in the nearest ½ of the image were included in transect counts. The density of organisms over a single transect was used as a sample unit for further analyses.

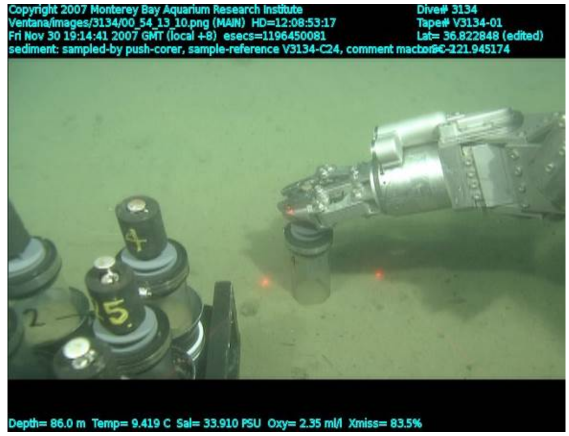

Figure 3. Collection of sediment push cores.

Sediment samples

Samples of seabed sediments for faunal and biogeological characteristics were collected using cylindrical (6.9 cm diameter) push cores which penetrated the sediment to a depth of ~20 cm (Fig. 3). The top 5 cm of each core sample (sediment volume = 187 cm^3) was washed gently through a 0.3 mm sieve using cold seawater. Collected organisms were relaxed using a 7% solution of magnesium chloride ($MgCl_2$), then preserved in a 4% formaldehyde (10% formalin) solution for several days. Samples were then rinsed with de-ionized water and stored in 70% ethanol for subsequent sorting and identification under a dissecting microscope. Samples from 2020 were both preserved and stored in 90% EtOH to allow for potential future macrofaunal molecular studies.

The grain size and organic carbon content of sediments were determined from push core samples. For each component a 1.1 ml subsample of the top 2 cm of sediment cores was collected using a 3 cc syringe bore (diameter = 0.84 cm). Grainsize fractions were measured by Moss Landing Marine Laboratories Geology Department, Moss Landing, CA. Organic carbon content was determined after acidification to remove carbonate minerals by the Dunbar Lab at Stanford University (through 2015) and by the Finney Lab at Idaho State University in 2020.

Local effects of cable installation

To assess the potential effects of the cable on local megafaunal assemblages, we compared the densities of animals living on versus off the cable path at 10 stations distributed evenly (5–6 km intervals) along the entire cable route (Fig. 2, orange triangles). At each cable station we determined the diversity and density of megafaunal along parallel 100 m^2 video transects, one over the cable route (impact) and the other 50 away (control).

Regional effects of cable installation

Variation in biological communities and the qualities of surficial sediments associated with and potentially caused by the installation and presence of the MARS cable were investigated at three depth regions corresponding to the principle habitats transited by the cable (Fig. 2). These include 1) the continental shelf (Shelf: < 200 m), 2) the continental shelf break and upper slope (Neck: 200–500 m) and 3) the continental slope region near the MARS benthic node (Slope: > 500). Within each region, a single cable station was selected on the cable route (impact), and three control stations were selected at distances of 1–16 km from the cable route (control, Fig. 2).

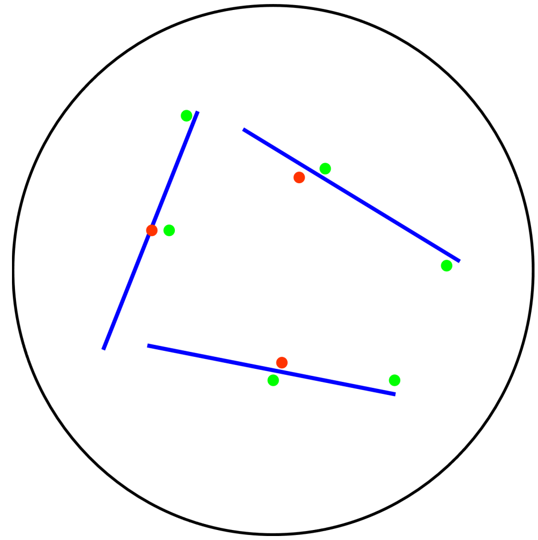

Figure 4. Sampling protocol for cable and control sites at each depth. Circle: 200 m-diameter station. Blue lines: 100 m^2 video transects. Green circles: sediment core samples for macrofaunal assemblage characterization. Red circles: cores for sediment characteristic measurements.

Each regional sampling station was defined as a 200-m-diameter circular area within which three replicate 100 m^2 ROV quantitative video transects were performed along semi-randomly selected compass headings and based on local current and visibility conditions (Fig. 4). In addition, replicate sediment push cores were collected (Fig. 4) at semi-random locations along video transects at each station to characterize macrofauna (n = 6 cores) and sediment characteristics (percent organic carbon, grainsize composition; n = 3 cores).

Skate density at Neck cable region

An aggregation of Longnose skates (*Beringraja rhina*) observed during the 2008 cable survey suggested that they may have been attracted to the cable in a specific 600–m long area where the taut MARS cable spanned small scarps and bathymetric depressions at a height of 2–10 cm above the seafloor. To test the hypothesis that this species (and perhaps others) was more (or less) abundant near suspended portions of the MARS cable, three replicate ROV quantitative video transects (100 m^2) were performed along the affected portion of the cable in the Neck cable region, and compared to three similar control transects performed 50 m from the cable.

Analytical methods

Differences in sediment features and biologic parameters between cable and control stations from both before and after cable installation were evaluated using a BACI (Before-After, Control-Impact) analytical design (Hewitt et al., 2001; Stewart-Oaten et al., 1986; Underwood, 1994). Using this design, individual 2-factor [Period (before, after), Treatment (cable, control)] comparisons were performed using permutation statistics available with *PRIMER-7* and *PERMANOVA+* (v.7.0.10; www.primer-e.com). Additionally, Permanova was used to analyze multivariate and univariate biological and sediment data comparing each region for 1) treatment (cable vs. control) effect for each report period 2) period effect amongst sampling dates and 3) period x treatment effect over report periods (2008-2020).

Faunal assemblage data were analyzed at the level of individual species and for ecologically important faunal groups (e.g., order, family, class). For multivariate tests, all species or all taxonomic groups were analyzed for community structure. For some univariate tests, only the most abundant species (~>1% of total faunal density) or faunal groups (~>3% of total faunal density) were analyzed.

The density of megafauna (100 m^{-2}) and infauna (per core) were square root-transformed prior to analysis to increase homogeneity of variances among groups and to reduce the influence of very abundant species. Univariate tests were run for sediment characteristics (mean grain size and % organic carbon), with no transformation of raw data and Euclidean Distance as an overlap measure.

Macrofauna counts (# $core^{-1}$) were square root-transformed. Similarity matrices for Permanova were calculated using Bray-Curtis for multivariate tests, univariate tests, and non- metric multidimensional scaling (nMDS) analysis.

For analyses using a large number of individual statistical tests, the probability (α) of a type I error (i.e., finding a significant difference between groups when it truly does not exist) increases. While α is usually set at 0.05 (95% confidence of avoiding type 1 error), it is often adjusted downward based on the number of tests performed to reduce the likelihood of type I errors (Cabin and Mitchell, 2000). This method may be effective for correcting type 1 errors, however its use is questionable (Cabin and Mitchell, 2000; Perneger, 1998) because it also increases the likelihood of type II errors (i.e., finding no difference between groups that truly differ). For this reason, α was maintained at 0.05 regardless of the number of tests used for analyses of cable impact data.

RESULTS and DISCUSSION

ROV impact surveys

In addition to surveying the 60 km length of the cable route six times, the field and analysis team completed 264 quantitative video transects (Appendix 1), and collected and analyzed 436 sediment cores (295 for macrofaunal analyses, 141 for sediment characteristics).

2008

A total of 16 days and 19 ROV dives with R/V *Point Lobos* and ROV *Ventana* were undertaken to complete the first MARS cable environmental studies from November 30, 2007 to April 1, 2008 (Appendix 1). Three additional sea days were cancelled or postponed due to weather or the presence of surface floats marking crab fishing gear, which interfered with ROV safety operations.

2010

The 2010 cable survey was performed between January 8, 2010 and April 9, 2010 during 11 sea days and 19 ROV dives. Shallow stations were sampled using the R/V *Point Lobos* and ROV *Ventana.* Deeper stations were surveyed using the R/V *Western Flyer* and ROV *Doc Ricketts* (Appendix 1). Three sea days were aborted due to severe weather conditions and some dives were cancelled or aborted early due to poor visibility or the presence of crab pots. Low visibility near the seabed was frequently caused by suspended sediment from river outflow after rain.

2015

The 2015 cable survey was performed between December 16, 2014 and December 18, 2015 during 10 days at sea and 19 ROV dives. Shallow stations were sampled using the R/V *Rachel Carson* and ROV *Ventana*. Deeper stations were surveyed using the R/V *Western Flyer* and the ROV *Doc Ricketts* (Appendix 1). Low visibility near the seabed was caused by suspended sediment at the shallower end of the cable route.

2020

The most current 5-year sampling season began on November 20, 2019 and was completed February 20, 2020. We used the R/V *Rachel Carson* and ROV *Ventana* for extended-length (12-hour) days to complete the survey over 11 days and 25 ROV dives (Appendix 1). During this investigation, crab season was unexpectedly delayed and the unusual presence of commercial traps on the seabed at Station D and along the shallower portion of the cable route (from Station I shoreward) through February 2020 prevented safe deployment of the ROV on numerous occasions (Fig. 2).

Cable and seabed condition

Seven general substrates, ranging from sand and mud to rocky habitat, were encountered along the MARS cable route. More than 76% of the route was composed of sand and sandy mud (Fig. 5, Table 1).

Table 1. Substrate composition on the MARS cable route, reported as total distance and as a percent of total distance.

Substrate	Distance (km)	Percent of route
Mixed substrate (mud and rock)	0.61	1.1
Mud	3.52	5.6
Mud over clay	7.80	12.7
Rippled sand	29.20	45.5
Rocky habitat	2.30	3.7
Sand	6.20	10.3
Sandy mud	10.37	21.1
Total	**60.00**	**100.0**

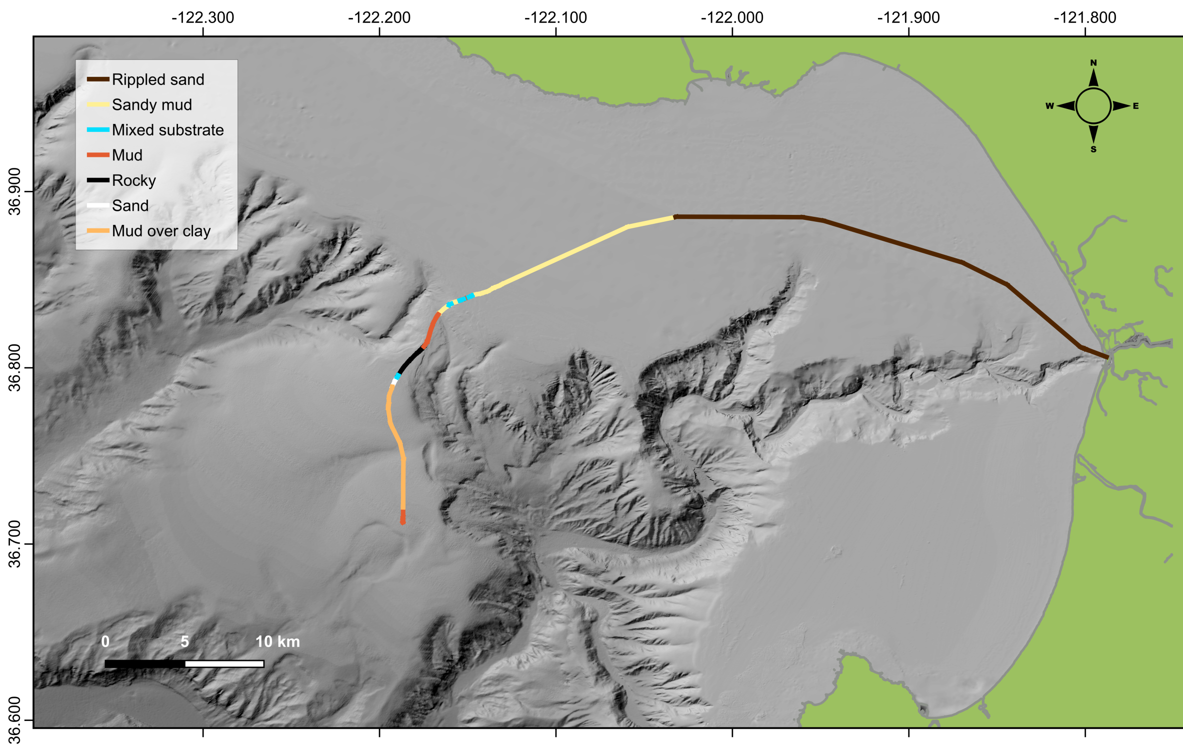

Figure 5. Substrate composition along the MARS route.

Exposed cable

During installation, it was not possible to bury (jet-in) the cable along the neck of Smooth Ridge between 116–453 m depth where rock and authigenic carbonate pavement is common. During the PLIB just weeks after it was installed in 2007, most of the cable (79%) was buried, 19% was exposed and 2% was partially buried (Fig. 6, Table 2). The majority of the cable, where buried, was 0.6–1.0 m below the seabed. Mean burial depth for the entire route, excluding where the cable was surface laid, was 0.94 m (Barry et al., 2007). Burial depth was underestimated in areas where an open trench did not immediately fill in with sediment.

During the PLIB, the cable was covered in sand at the beginning of the route and neither it, the cable trench, nor any habitat disturbance was visible for a distance of more than 34 km. This portion of the route is remains buried and the cable was visually undetectable through 2020 (Appendix 2, Fig. A). Where the cable was exposed, 95% of it rested on the seafloor (Table 3; Appendix 2, Fig. B). In 2008 there appeared to have been some minor redistribution of the tension in the cable. From 120–300 m depth, sections of the surface-laid cable were sinking into surficial sediments. As now-filled trenches (Appendix 2, Fig. C and D) and previously exposed portions of the cable continue to settle into the mud, the proportion of the cable that is buried has risen in 2020 to 87.3%. The remainder (12.7%) is exposed, intermittently exposed, or shallowly buried (Table 2). Along a 7.6 km section between 116–453 m water depth, the cable is still exposed, shallowly or intermittently buried (Fig. 6, Table 2). The cable is fully buried along the final 9 km of its route, and emerges a few meters from its termination at the seaward MARS node (891 m depth; Appendix 2, Fig. E). The 2020 survey established that 87% the cable is buried beneath the surface of the seabed, with 95% of the exposed cable resting on the seafloor (Table 3).

Table 2. Condition of the MARS cable along the route, reported as total distance and as a percent of total distance. Comparison from 2007 post-lay inspection and burial through 2020 results are shown.

	Buried		**Exposed, intermittently exposed, or shallowly buried**	
Survey	Distance (km)	% route	Distance (km)	% route
PLIB 2007	47.4	79.0	12.6	21.0
2008	49.3	82.2	10.7	17.8
2010	51.6	86.0	8.4	14.0
2015	52.4	87.3	7.6	12.7
2020	52.2	87.0	7.8	13.0

In early surveys, no evidence of trawling impact on the main cable was observed, nor was any major change apparent along exposed portions of the cable. There was no evidence of strumming or other movement of the cable. In 2009–2010 the area around the MARS node was trawled at least three times and localized damage occurred to small auxiliary cables and instrumentation near the node, but not to the cable or node itself (Appendix 2, Fig. F). Currently, a 1300 m-long section of exposed cable on the neck of Smooth Ridge is displaced to the SW at a maximum distance of 135 m (Fig. 6, inset). We are unsure of exactly when or how the cable was moved, but suspect a trawling incident.

Major spans or point suspensions in the MARS cable were not observed in any cable surveys, even after this movement of the cable. In numerous short sections, the cable is still 1–6 cm above the seafloor, as the cable is being pulled taut where the seafloor is slightly irregular due to rocks or minor bathymetric heterogeneity (Appendix 2, Fig. G). Such irregularities also resulted in minor point suspensions (Appendix 2, Fig. H) and minor spans (Appendix 2, Fig. I) up to 55 m long, caused by rocks and ledges in this region (Fig. 6, Table 3). The highest are 1.2 and 0.5 m above the seafloor for a distance of 49 and 54 m (Appendix 2, Fig. J); all others are at a height of 0.2 m or less (Table 6). In all, fewer minor spans and point suspensions were observed along the route than in 2007 (79 in 2007, 26 in 2020, Table 6).

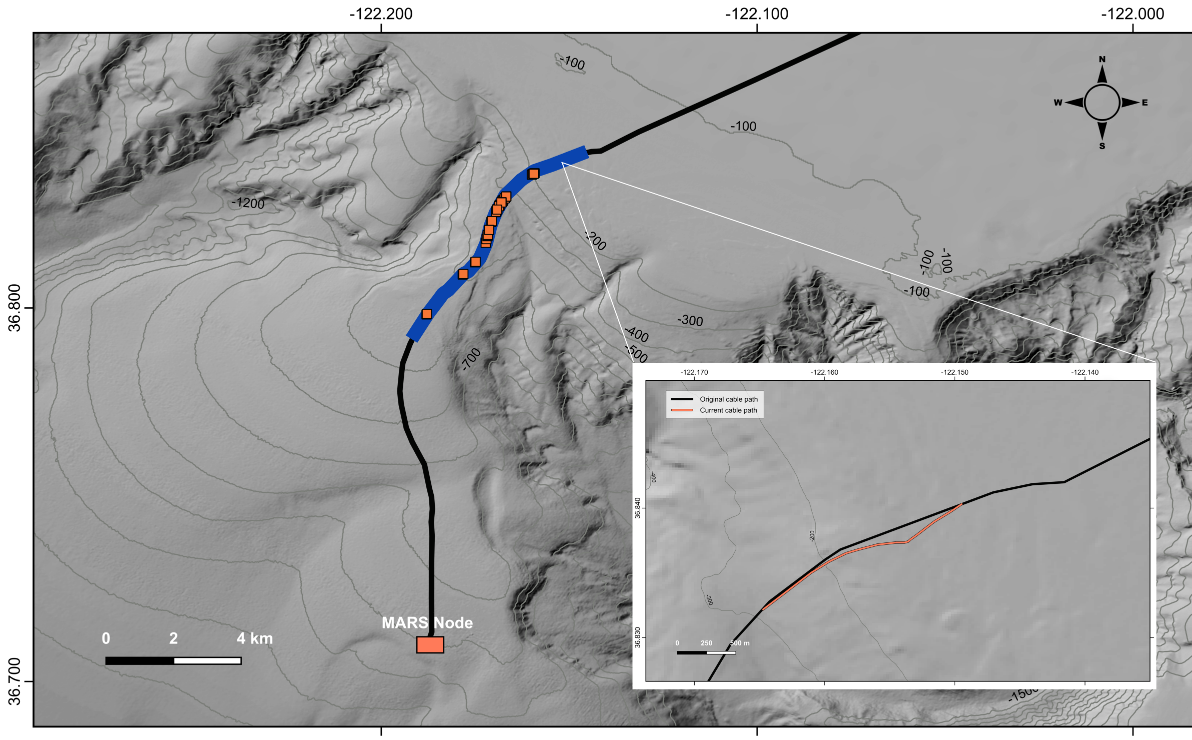

Figure 6. The MARS cable is buried along the entire route except for the area on the neck of Smooth Ridge, shown in blue. In 2020, the cable was 87% buried with 13% either exposed, partially buried or shallowly buried. Spans of the cable, as a result of minor topographic changes and rocks, are shown as orange markers within the area where the cable is exposed. Inset: A section of the cable has moved a maximum of 135 m to the SW, likely due to a trawling incident; the exact time frame for which this occurred is not known.

Table 3. Number and extent of minor spans/suspensions in the exposed portion of the MARS cable along the neck of Smooth Ridge; initial PLIB position compared to the most recent survey. No major spans or suspensions occurred. The first category represents "point suspensions", where the cable is less than 20 cm above the seafloor for a short distance. Spans are areas where the cable is above the seafloor for the given distance are caused by rocks and other or topographic highs in the surficial geology.

Type	2007		
	Number	Height (m)	Length (m)
Point susp.	68	< 0.2	< 4
Span	1	0.08	8
Span	1	0.08	12
Span	1	0.08	13
Span	1	0.08	128
Span	1	0.08	159
Span	1	0.09	10
Span	1	0.15	9
Span	1	0.15	16
Span	1	0.15	18
Span	1	0.15	27
Span	1	0.50	16
Span	1	1.20	25
Total	79		abt. 577
Type	2020		
	Number	Height (m)	Length (m)
Point susp.	11	< 0.2	< 4
Span	1	0.05	12
Span	1	0.05	17
Span	2	0.08	13
Span	1	0.08	18
Span	1	0.08	23
Span	3	0.08	27
Span	1	0.08	37
Span	1	0.08	40
Span	1	0.08	55
Span	1	0.10	19
Span	1	0.50	54
Span	1	1.20	49
	26		abt. 386

Habitat Disturbance

Following its installation in 2007, a deeper section of the cable was exposed in an open, clay-lined trench and was categorized as unburied (Appendix 2, Fig. C). The cable trench gradually filled with soft, lighter-colored sediment and by ~2010, had completely infilled (Appendix 2, Fig. D). Other sections of the cable installed without trenching were resting on the seafloor (2008) and are now (2020) covered with 5–60 cm of sediment. While there are changes to the amount of sediment under the end points of some spans (build up or erosion), they are essentially the same in 2020 as was observed in earlier surveys. In several locations, fine sediments have winnowed from beneath the cable leaving large grain sizes (Appendix 2, Fig. K).

The cable installation plow caused disturbance in habitats where sediment is underlain by authigenic carbonate rock. The plow brought blocks of sediment to the surface, forming new heterogeneous habitat. Sediment surrounding these rocks has since winnowed, leaving the carbonate exposed (Appendix 2, Fig. L).

Where the cable remains exposed, the number of sessile animals (mostly anemones and crinoids) attached to the cable increased up to 2015, and stabilized by 2020 (Table 4).

Table 4. Use of the MARS cable as habitat over time. Sessile and semi-sessile animals along with the approximate number of individuals attached to the cable. Impact surveys and the number of years since cable installation are shown.

		Survey year (years since installation)			
		2008 (1.5)	2010 (3)	2015 (8)	2020 (13)
Organism	**Mobility**	**Number of Individuals**			
Florometra serratissima (crinoid)	semi-sessile	7	108	1022	843
Liponema brevicorne (anemone)	semi-sessile	39	345	882	6
Psolus squamatus (sea cucumber)	semi-sessile	0	0	0	5
Actinostolid/Hormathid (anemone)	sessile	0	189	1037	586
Metridium farcimen (anemone)	sessile	13	37	292	842
Porifera (sponge)	sessile	0	0	84	590
Corallimorphus pilatus (corallimorph)	sessile	0	0	10	15
Heteropolypus ritteri (soft coral)	sessile	0	0	4	35
Total		**59**	**679**	**3331**	**2922**
Ephemeral attachments:					
Eggcase (*Pleurobranchaea californica*)		4	0	0	2
Eggcase (elasmobranch)		0	0	100's	100's

Sediment characteristics

Sediment grain size and organic carbon content varied between treatments, stations, and sampling dates for all three cable regions. Because sediment samples were not collected before the cable was installed, variation in sediment characteristics among control and cable stations may represent natural variation or the effects of cable installation or both.

Sediment grain size

Mean sediment grain size ranged from 3–289 µm, with the coarsest sizes at Slope stations in 2010 (mean = 172 µm, Figure 7). Finer mean sizes characterized the Shelf (mean = 44 µm in 2008).

Grain sizes at Shelf stations varied significantly over the sampling periods, between cable and control stations, and for treatment x period (all p = 0.001). In 2008, mean grain sizes were significantly smaller at the control stations than at the cable station (p <0.001; Figure 7), which might be expected in association with the installation of the cable. In 2010 and 2015 mean grain size did not differ significantly between the cable and control stations. In 2020 grainsize was larger at the cable station (p = 0.026). The effects of the cable on sediment grainsize, if any, are smaller than the range of natural variation among stations and through time.

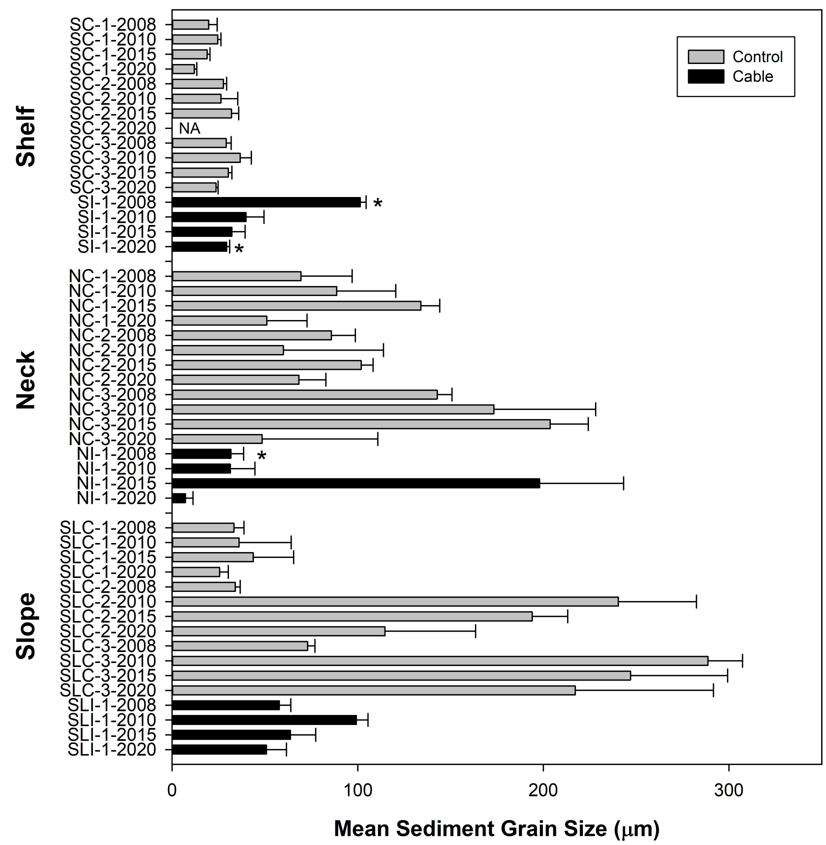

Figure 7. Mean sediment grain size (+/- SD) at control and cable stations for cable regions. * = significant difference between control and cable areas for the specific sampling periods.

Observations of sediment winnowing are common along the heterogeneous bottom in the Neck region, compared to the smooth, sediment-dominated seafloor typical of shallower Shelf, and deeper Slope regions. Sediment grain size in the Neck region varied significantly among sampling periods (p = 0.001). Grainsize was significantly smaller for cable samples compared to controls in 2008 (p = 0.005) and differed over all sampling periods (p = 0.034); period x treatment was also significant for all sampling periods, p = 0.041.

Interstation variation in grain size was observed at the Slope region. Overall, there was no significant difference in mean grainsize between sampling dates. There was a significant treatment effect between control and cable treatments over all sampling dates (p = 0.044).

Sediment organic carbon content

The organic carbon content of sediments varied considerably, ranging from 0.35–1.33 percent, with most organic-rich sediments generally found in the finer grain sizes at SC-1 on the shelf. No differences in the percent organic carbon of sediments were detectable among years (2008–2020) or among depth regions (p > 0.05).

The organic carbon content of sediments in the Shelf region did not differ (p > 0.05) among cable and control sites for any survey year (Fig. 8). In the Neck region, sediments at cable stations had a higher percentage of organic carbon in 2008 (p = 0.04), 2010 (p = 0.01), 2015 (0.02), but not in 2020 (p = 0.1). Similarly, cable stations in the Slope region had higher carbon content in 2010 (p = 0.02) and 2015 (p = 0.01), but not in 2008 nor 2020 (p > 0.05).

Organic enrichment at cable stations could represent natural variability or enhancement of organic-rich materials (e.g., aggregation of debris or organisms) due to the presence of the cable or burial trench. The Slope cable station is located near the MARS node, where frequent ROV visits supporting science operations may cause minor disturbance, potentially enhancing the amount of organic debris present.

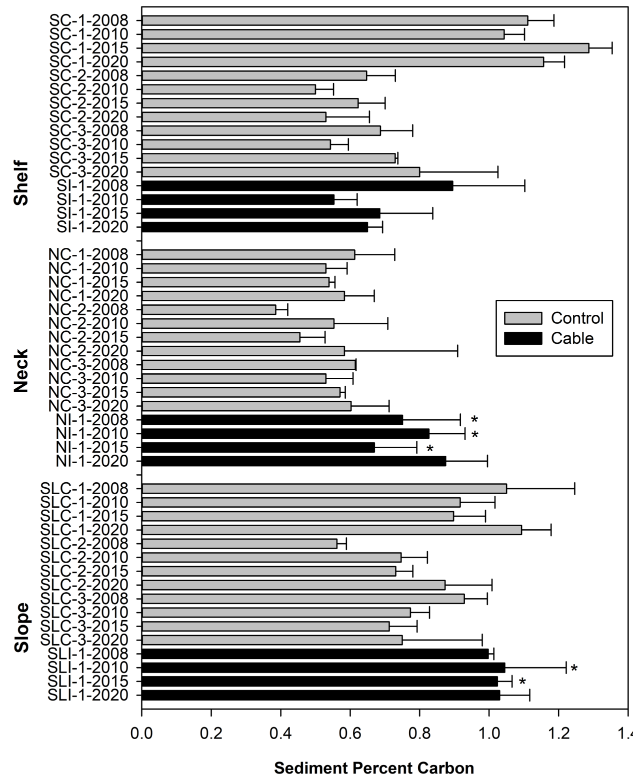

Figure 8. Mean percent organic carbon in surficial sediments for control and cable sites at the three cable depth regions (+/- SD). Comparisons of control vs. cable sites was nonsignificant for the Shelf region. Differences were significant for Slope and Neck regions during some, but not all sampling periods. * = significant difference between control and cable areas for the sampling period.

Megafaunal assemblages

Benthic megafaunal assemblages were characterized from 261 quantitative video transects for which we observed 39,767 individual organisms from 155 taxa (Fig. 9, Appendix 1). The overall mean density of megafauna was 160 ind. 100 m^{-2} (Table 5). Cnidarians, particularly sea pens (Pennatulacea, Fig. 10) and anemones (Actinaria) were most abundant groups, comprising almost 50 percent of total megafaunal density. Echinoderms ranked second among phyla with 27 percent of the total density, particularly seastars (Asteroidea) and urchins (Echinoidea), and, Table 5). Fishes (Vertebrata) were the third most abundant phylum with 9 percent of the total density; flatfishes (Pleuronectiformes) and rockfishes (Sebastidae) had the highest densities amongst the vertebrates.

The top five ranking megafaunal species accounted for 63% of total density. *Funiculina* sp., a common sea pen at slope depths near 500–1000 m was the most abundant species (22 ind. 100 m^{-2}), and 16.3 % of total megafaunal density. Sea pens (likely *Acanthoptilum* sp.), were very common on the continental shelf (10.9 % of megafauna), and *Stronglylocentrotus fragilis,* a common urchin at upper slope depths, accounted for 13.0% of total density in 2020. This species is known to form ephemeral aggregations, and densities vary widely over time.

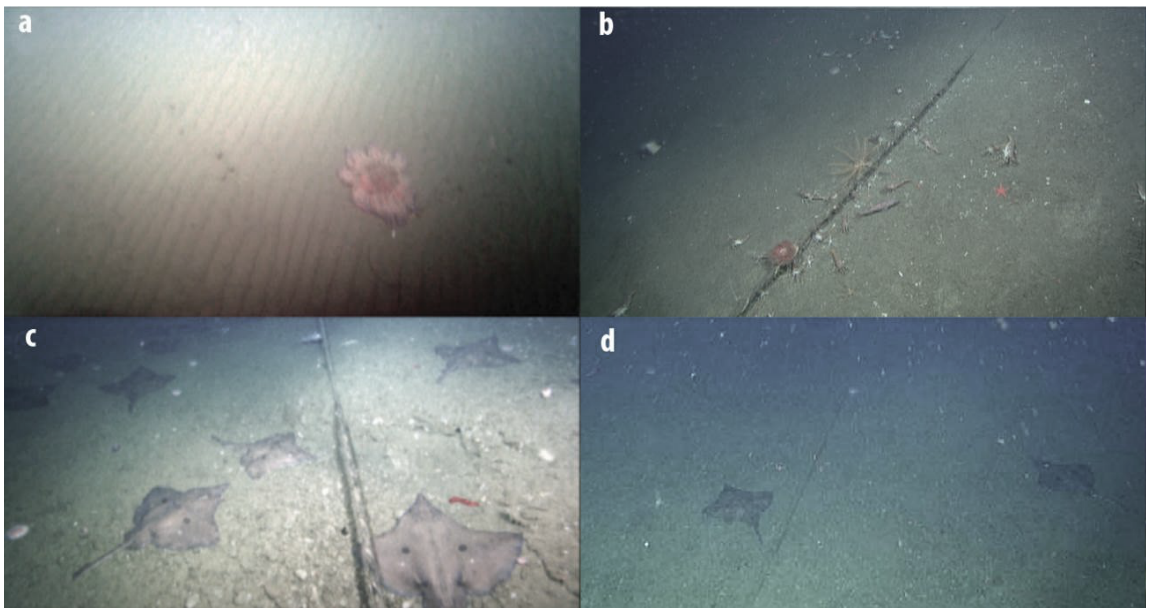

Figure 9. Megafauna along the cable route. A. Sand ripples and the seastar *Pycnopodia helanthoides* at 31 m depth where the cable is buried and no habitat disturbance is visible. B. Cable on seabed at 226 m depth with an anemone and crinoid attached. C. Skate (*Beringraja rhina*) aggregation at 303 m depth in early 2008 near the unenergized cable. D. Far fewer skates were present in this area after the cable was energized in 2010.

Table 5. Summary of megafaunal density by phylum and group for all regional and localized station transects over time (n = 249). Density is listed as the mean (100 m^{-2}), standard error of the mean (SE), and percent of total density (%). See also Appendix 3 for densities of animals found at control stations only.

Phylum	Group	Mean	SE	%
Cnidaria		**79.20**	**15.73**	**49.59**
	Pennatulacea	53.01	10.01	33.19
	Actiniaria	20.74	4.28	12.99
	Ceriantharia	4.86	1.23	3.04
	Alcyonacea	0.37	0.15	0.23
	Corallimorphidae	0.19	0.05	0.12
	Anthozoa	0.01	0.01	0.01
	Rhodaliidae	0.02	0.01	0.01
Echinodermata		**43.74**	**11.13**	**27.39**
	Asteroidea	16.76	2.02	4.51
	Echinoidea	14.44	2.43	9.04
	Holothuroidea	6.28	4.99	9.91
	Ophiuroidea	6.04	1.59	3.78
	Crinoidea	0.22	0.1	0.14
Vertebrata		**14.17**	**3.33**	**8.88**
	Pleuronectiformes	5.91	1.09	3.70
	Sebastidae	3.69	1.00	2.31
	Zoarcidae	1.66	0.40	1.04
	Hexagrammidae	0.58	0.10	0.36
	Actinopteri	0.47	0.13	0.29
	Agonidae	0.45	0.08	0.28
	Myxinidae	0.22	0.05	0.14
	Merlucciidae	0.20	0.07	0.13
	Stichaeidae	0.19	0.09	0.12
	Squalidae	0.18	0.05	0.11
	Rajiformes	0.15	0.05	0.10
	Liparidae	0.13	0.05	0.08
	Embiotocidae	0.10	0.04	0.06
	Macrouridae	0.08	0.04	0.05
	Anoplopomatidae	0.06	0.02	0.04
	Scyliorhinidae	0.05	0.03	0.03
	Moridae	0.03	0.01	0.02
	Torpedinidae	0.01	0.01	0.01
	Alepocephalidae	0.00	0.00	0.00
	Chimaeridae	0.00	0.00	0.00
Mollusca		**9.38**	**2.83**	**5.88**
	Gastropoda	7.62	2.15	4.77
	Cephalopoda	1.30	0.27	0.81
	Bivalvia	0.47	0.41	0.29
Annelida		**6.36**	**2.05**	**4.22**
	Polychaeta	4.97	1.68	3.11
	Echiura	0.10	0.04	0.06
	Sabellidae	0.41	0.12	0.255
Arthropoda	Decapoda	**5.36**	**2.11**	**3.36**
Porifera		**2.25**	**0.59**	**1.41**
Tunicata		**0.08**	**0.04**	**0.05**
Brachiopoda		**0.05**	**0.03**	**0.03**
Total		**159.71**	**37.62**	**100.00**

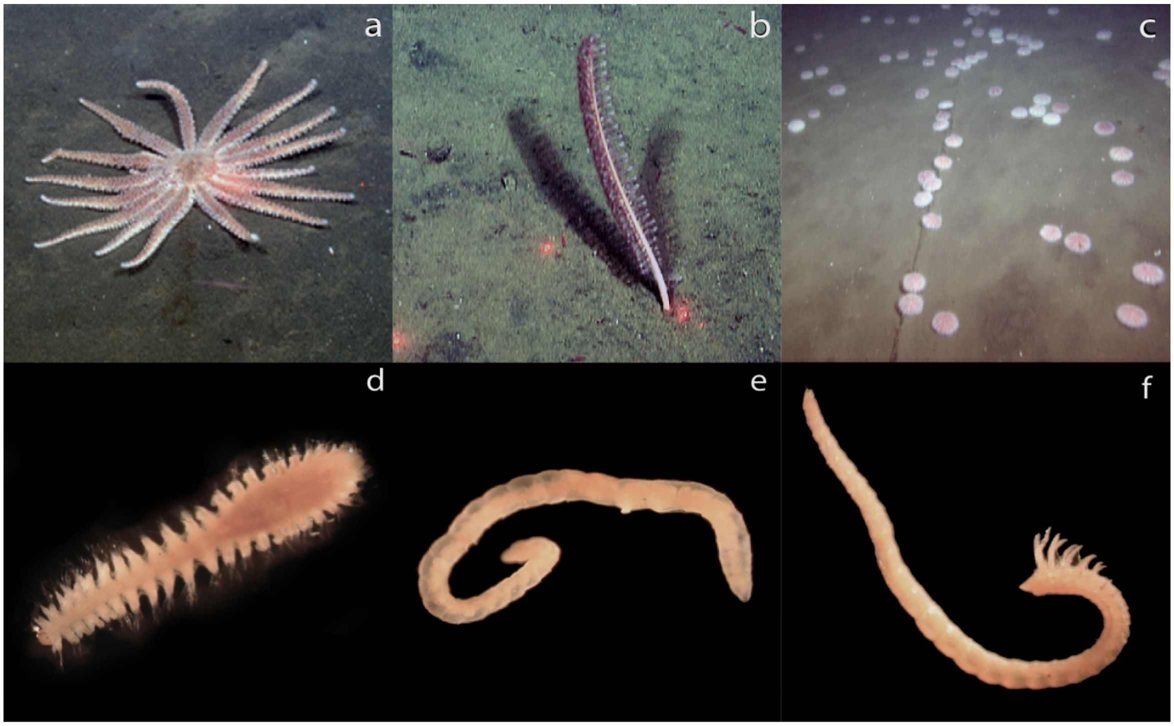

Figure 10. Some of the most abundant megafaunal and macrofaunal animals along the MARS cable route. A–C: Megafauna (ROV video transects): A. *Rathbunaster californicus* (sea star). B. *Funiculina* sp. (sea pen). C. *Stronglylocentrotus fragilis*, (urchin). D–F: Macrofauna (sediment cores): D. *Cossura* sp. (polychaete worm). E. Oligochaeta. F. *Prionospio* sp. (polychaete worm).

Local effects of cable installation

Between 2008–2015, little variation in the megafaunal assemblage was detected between video transects at 10 stations directly over the cable route vs. transects parallel to the cable, but 50 m away (A-J, Fig. 2). Multivariate tests comparing cable and control treatments for all species or all groups were non-significant for investigations prior to 2020 ($p = 0.99$). Likewise, univariate tests detected no differences in the density of faunal groups or individual species on the cable route and 50 m away.

In 2020, we observed the first statistically significant difference in the densities of various taxa living on or near the cable at these 10 regional stations ($p = 0.003$ for period, Figure 11). High megafaunal densities at the cable were observed at the two stations where the cable is exposed. At Station B, sponge densities were much higher at the cable (86 vs. 11) and there were 32 actinostolid anemones attached to the it. Large numbers ($n = 439$) of the sea star *Rathbunaster californicus* (Fig. 10a) were present near the cable at Station C (Fig. 2), but none were observed on the transect 50 m away. There were also 54 *Stylasterias forreri* sea stars, and 22 sea cucumbers (*Apostichopus leukothele*) near the cable. Twenty-four anemones (*Metridium farcimen*) are now attached to the cable at this station. Also for the first time, we observed almost 1600 individual dead and dying midwater pyrosomes on the seafloor along the cable route. At station C, *R. californicus* was observed feeding on pyrosome detritus that had accumulated along the cable.

A notable anomaly in faunal abundance occurred in 2008 near 300 m depth in the Neck depth region where aggregations of Longnose skates (*Beringraja rhina*) were observed along short sections where the cable was taut between rocks and suspended 2-10 cm above the seafloor (Fig. 9c). At this time, the cable was not yet energized. Based on this anomaly we added an 11th temporary regional station to expand sampling for this phenomenon. The mean density of *B. rhina* along the cable (33 100m^{-2}) was far higher than in nearby control areas (0.3 100m^{-2}; $p = 0.027$). The densest aggregations were concentrated along a 75–100 m section where the skates were resting on the seafloor within 5–10 m of the unpowered cable. We also noted somewhat higher than normal numbers of the elasmobranchs *Parmaturus xaniurus* (catsharks) and *Hydrolagus colliei* (spotted ratfish) in this general area of the cable route, but off the quantitative transect. During the subsequent cable survey in 2010 after the cable was energized, skate densities were lower overall and did not differ ($p = 0.90$) between cable (9.7 100m^{-2}) and control (6.3 100m^{-2}) locations (Figure 9d). Nor did the density of other elasmobranchs in the area appear to vary in association with the cable. As in 2010, the abundance of elasmobranchs was not elevated near the powered cable in 2015 or 2020.

None of the amassed Longnose skates were observed feeding or mating and we know of no mating or feeding aggregating behaviors in this species. A number of marine fishes, especially elasmobranchs are known to sense electromagnetic fields using electroreceptors as a method of prey detection (Bullock, 1982). Sea urchin embryos, *Tritonia diomedea,* skates, rays, sharks and some bony fishes sense electric fields using specialized organs, providing information related to prey detection, navigation, or the detection of conspecifics and predators (Normandeau et al., 2011). A weak electromagnetic field was likely generated around the suspended MARS cable by induction as local ocean currents flow through the Earth's magnetic field and around the cable (Slater et al., 2010). This is possible even though the cable was not energized during the 2008 video survey. We note that although taut cable sections were observed in several areas along its route, skate aggregations were only observed in one location, for unknown reasons. The combination of bathymetry (small scarps and sediment depressions unique to this area), the natural distribution of the animals, and a mild electrical field may have contributed to the aggregation. Electric fields from telecommunications cables and power distribution cables (e.g., coastal windfarms) are expected to have ecological effects due to their effects on the behavior of various species capable of electroreception (Gill, 2005; Gill et al., 2012; Slater et al., 2010; Snoek et al., 2016).

Love et al., 2017 found that EMF's near an energized cable in southern California fell to background levels within 1 m of the cable. In this study the density and species composition of invertebrates and bony fishes along unenergized cables did not differ from nearby energized cables. Although the power status of the cable appeared to play little role, fishes and invertebrates were more abundant in cabled areas (regardless of power status) than in uncabled control areas. As we observed along the MARS cable, the introduction of hard substrata (e.g., cables) provides habitat for sessile invertebrates largely unavailable in sediment dominated environments (e.g., the anemone *M. farcimen*) (Kogan et al., 2006; Love et al., 2017). Fishes may be attracted to increased spatial heterogeneity in a habitat as a means for predation avoidance, or increased feeding success (Mikheev et al., 2010).

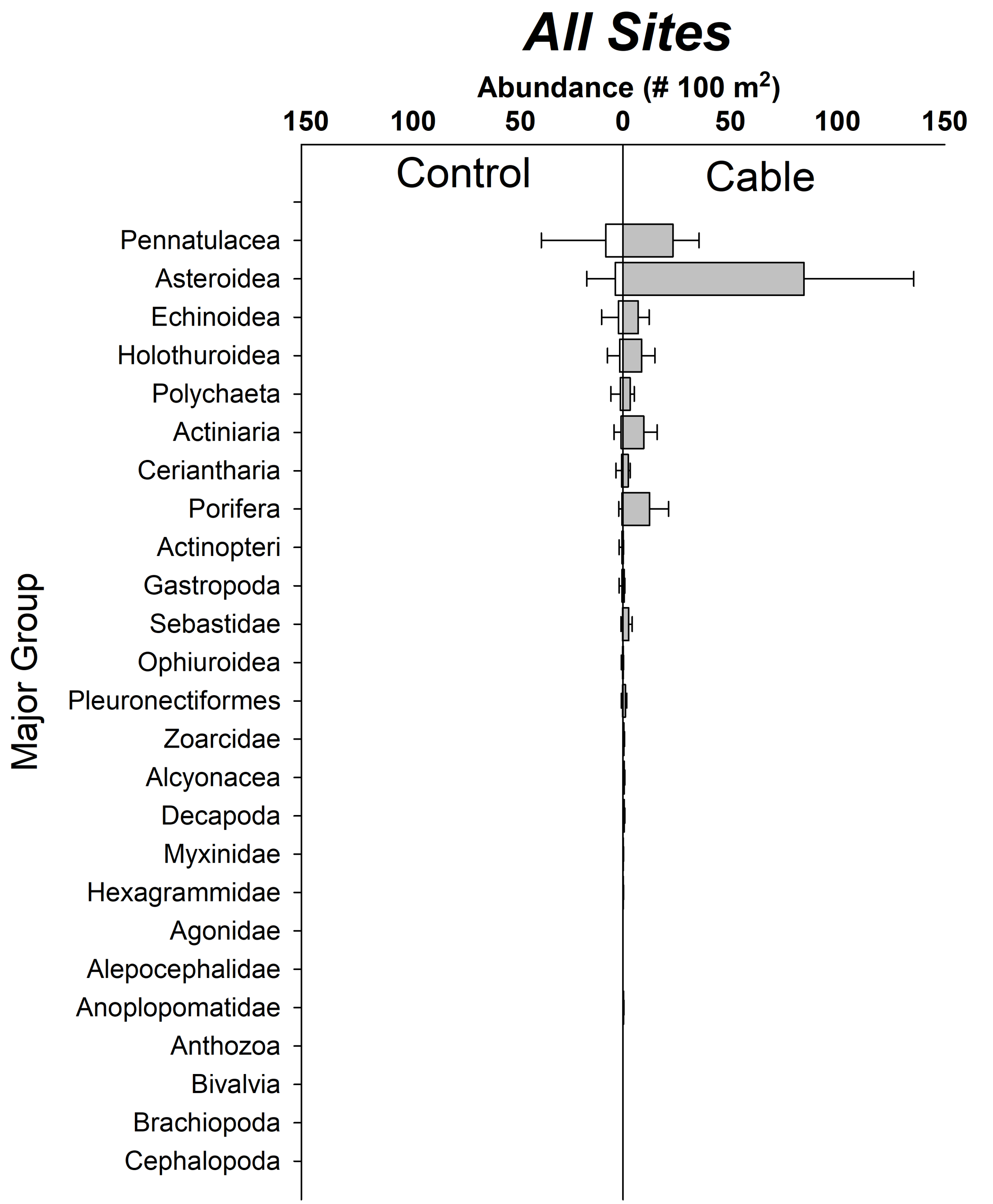

Figure 11. Variation in mean density for the top 25 megafaunal groups at local stations along the cable route for the 2020 sampling period. Paired transects for all prior sampling dates showed little variation in the types and densities of megafaunal taxa over 10 sites along the cable ($p = 0.99$ in 2015). In 2020, densities for groups at cable sites were significantly higher than at control sites ($p = 0.03$). Changes at the two stations where the cable is exposed accounted for the differences. Cable = directly over the cable route. Control = 50 m away from, and parallel to the cable, error bars = SEM.

Regional effects of cable installation

The installation and presence of the MARS cable appears to have mild to benign effects on the structure of the megafaunal assemblages over a scale of kilometers, based on the results of samples from cable and control stations before and after cable installation. Multivariate and univariate analyses indicate that natural variation in megafaunal assemblages over space and time is equal or greater than any influence of the cable or its installation. Changes in community structure with depth are by far the largest source of variation, illustrated clearly in the clustering of stations in three main groups representing Shelf, Neck, and Slope regions (Fig. 12). Any influence of the cable is minor or at most masked by natural variability in megafaunal assemblages within depth regions or at individual stations, shown by the intermingled clusters of control and cable stations in Fig. 12.

BACI analyses used to evaluate changes related to the presence of the cable, a significant effect of cable installation would be indicated by a statistically significant Period x Treatment (PxT) interaction term for the density of a particular taxon (for univariate or multivariate tests). This result would indicate that any change in the density of the taxon between periods (i.e., *Before* and *After* cable installation) at the cable stations was different than changes in density at control stations.

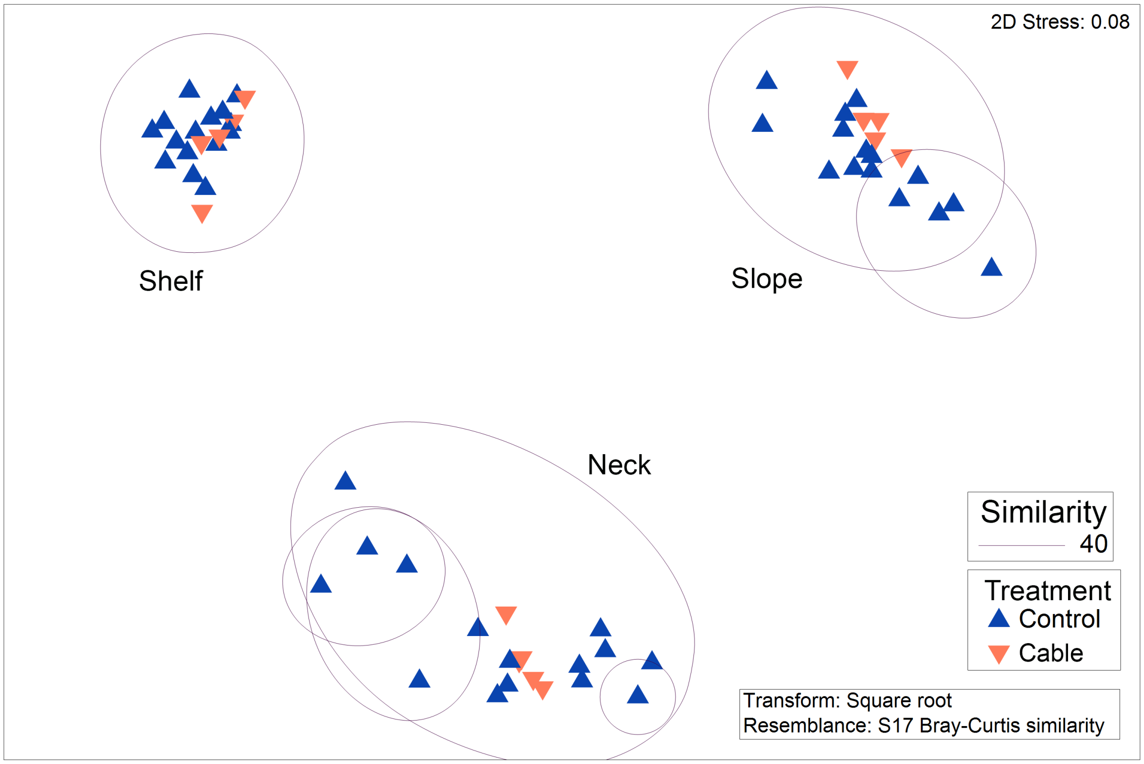

Figure 12. nMDS plot based on Bray-Curtis Similarity Index (community species richness and densities). Regional megafaunal communities remained at least 40 percent similar in a comparison of community structure based on cable stations and control stations. Stations clustered based on depth, with Shelf, Neck and Slope regions most similar to each other. Cable stations cluster within the natural variation at control stations, indicating no major effects of the cable. Permanova results for period, treatment and period x treatment interaction were not statistically significant.

Few changes in the megafaunal community were attributable to the installation or presence of the cable at either the species/taxon or group levels (Table 6, Fig. 12–15). At Shelf, Neck and Slope regions, multivariate comparisons (i.e., comparisons between the entire megafaunal assemblage by species) indicated no overall significant PxT interaction terms (p = 0.94, 0.98, 0.98 respectively). Similarity of biological communities based on species richness and densities, remained distinct between Shelf, Neck and Slope regions over time (Fig. 12). Cable stations within individual regions were similar to control stations.

Multivariate analyses also indicated significant variation in megafaunal density associated with main factors (Periods or Treatments, or both). Combined with the non-significant interaction terms these results indicate that most variation megafaunal communities associated with natural variability between stations or periods – in other words, the scale of variation in megafaunal density among control stations was equal or greater than measured between control and cable stations.

Megafauna in the Shelf region (Fig. 13) varied among years ($p = 0.009$) but not in relation to the cable. Specifically, Asteroids (seastars, $p = 0.013$), Ophiuroids (brittle stars, $p = 0.007$) and Gastropods (marine snails, $p = 0.023$) varied significantly in density from 2007–2020. These taxa are mobile and known to fluctuate in density under natural conditions. Low water clarity in the nearshore stations was encountered frequently and could affect megafaunal counts along transects, with consequences for data analyses, especially for smaller animals. The sea star *Luidia foliolata* was unusually abundant in 2015 transects.

No significant variation in megafaunal communities were detected in the Neck region when all taxa were included in BACI analyses (Table 6). Univariate tests indicated that pleuronectiformes (flatfishes, $p = 0.027$ for treatment) were consistently more abundant at control stations than at the cable station in this region.

At the Slope region, the density of Pennatulacea (sea pens, $p = 0.027$ for treatment) fluctuated widely between cable and control stations. The densities of *Funiculina, Pennatula phosphorea and Umbellula lindahli* varied widely; each species was observed in high densities in 2015 at the cable station, but not at the three control stations. The density of all three species dropped to background levels at the cable station in 2020. Perhaps some unseen organic enrichment occurred between 2010–2015 as an effect of the cable or under natural circumstances, leading to a significant result for the cable station at the higher taxon group level ($p = 0.045$), and for period at the species level ($p = 0.024$; Table 6). The significant PxT interaction for holothurians (sea cucumbers, $p = 0.035$) was due a single large aggregation of *Pannychia moselyi* during initial biological characterization surveys at the cable station before the cable was laid (Table 6). Pleuronectiformes (flatfishes, $p = 0.028$ for period) were found in higher than normal numbers in 2010 at all control and cable stations, indicating natural variation or variation not related to the cable. Sebastidae (rockfish *Sebatolobus*) showed a significant difference for period ($p = 0.001$). High densities of these fishes were observed in 2015 and again in 2020 at both the cable and control stations in the Slope region. Natural variation or changes on bottom trawling may be factors. Anemones (Actiniaria, $p = 0.042$ for period) were particularly abundant between 2010–2015 at both cable and control stations.

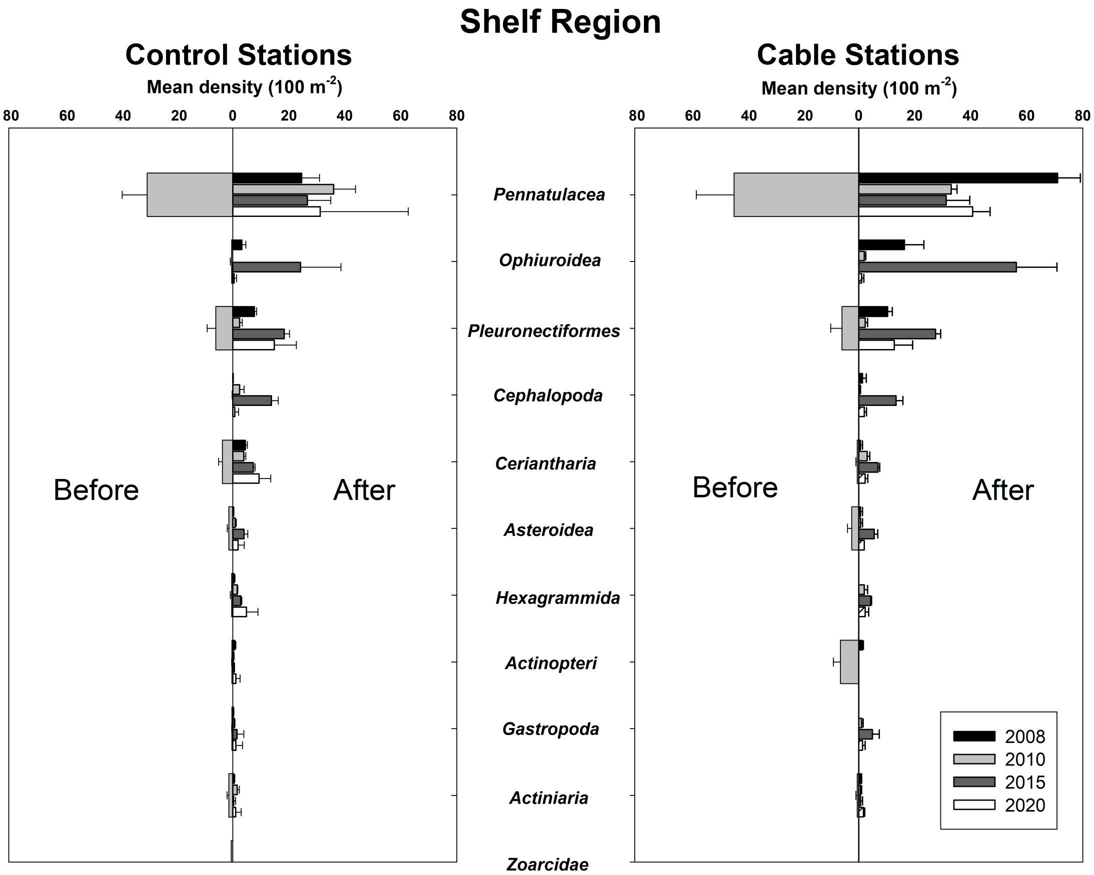

Figure 13. Variation in megafaunal density (by taxonomic group) among treatments and periods at the Shelf region. BACI analysis indicated significant changes in density over time ($p < 0.001$), but no overall significant effect of cable installation ($p > 0.05$) in this region for higher-level taxonomic groups. We observed significant changes in abundances of ophiuroids, asteroids, and gastropods over time, which is attributed to natural variation due to normal species aggregations. Error bars = stand error of the mean.

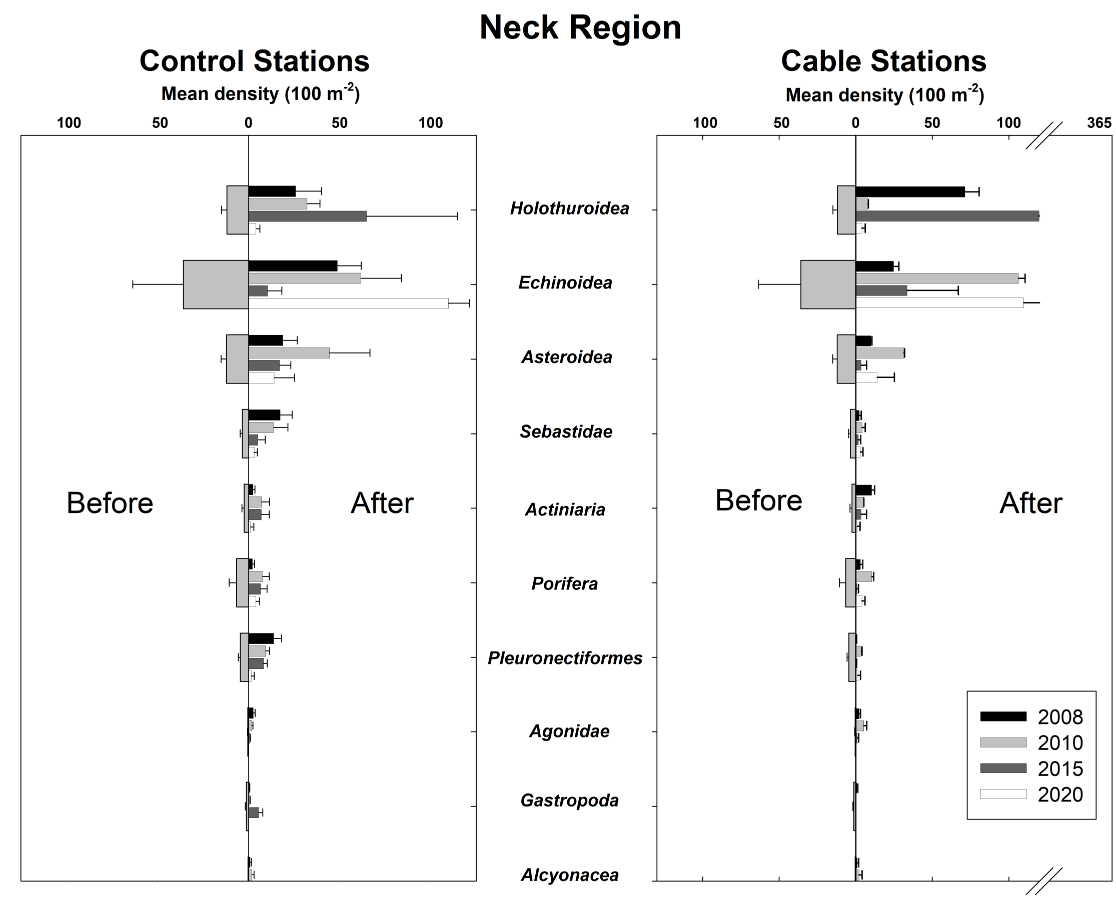

Figure 14. Variation in megafaunal assemblage by taxonomic groups combined among periods and treatments at the Neck region. BACI analysis indicated no significant effect of cable installation for density changes over time, for treatment, nor for PxT interaction. There was an effect of treatment for flatfishes (Pleuronectiformes), with more at control stations vs. near the cable. Error bars = standard error of the mean.

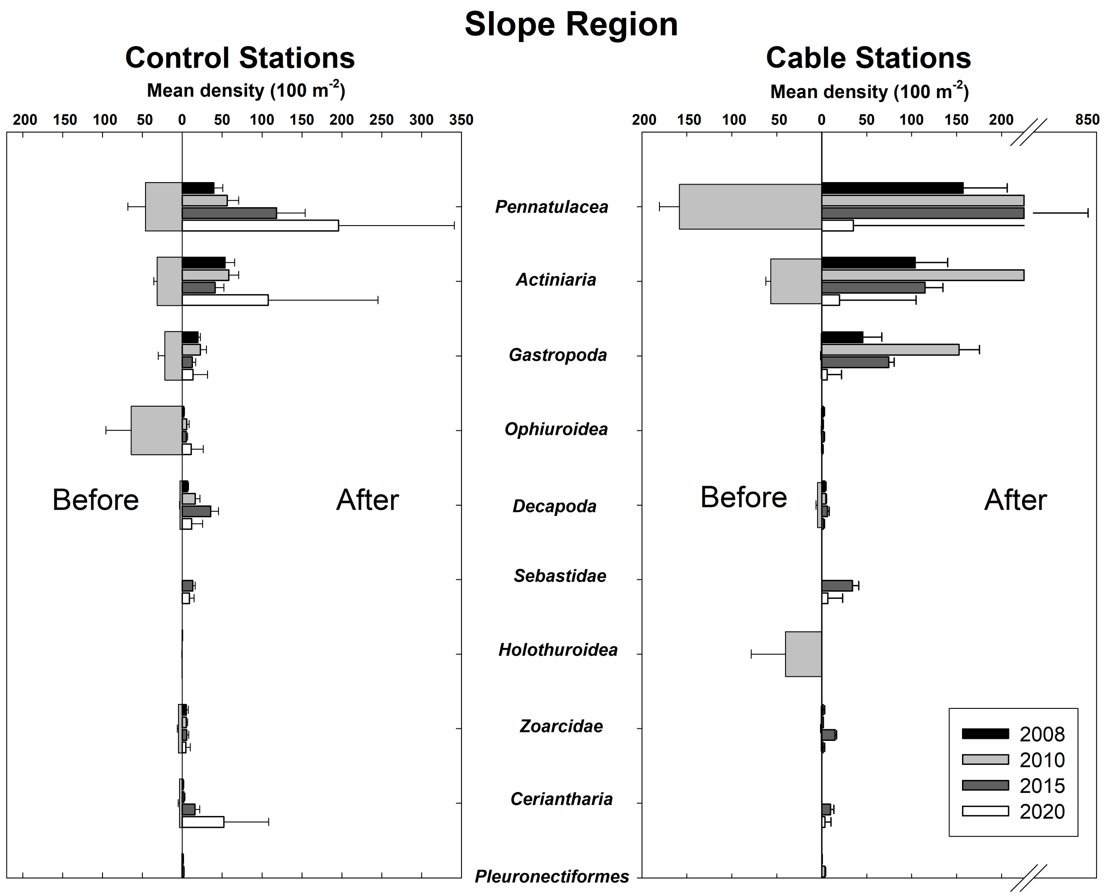

Figure 15. Variation in megafaunal assemblage among periods and treatments at the Slope region. BACI analysis indicated no density changes over time (p >0.05), but an overall significant effect of cable installation (p <0.001) in this region. There was a treatment effect for sea pens (Pennatulacea), and anemones (Actiniaria) with higher densities at cable stations. Sea cucumbers (Holothuroidea) was significant for period, treatment and PxT due to a large natural aggregation at the cable station in 2008. The density of Sebastolobus rockfish (Sebastidae) and flatfishes (Pleuronectiformes) changed over time, with increases in 2015 and 2020 at control and cable stations. Error bars = standard error of the mean.

Table 6. Summary of multivariate and univariate BACI analysis for megafaunal taxa for all cable regions and periods. P= Period, T= Treatment, PxT = Period x Treatment interaction term. A significant PxT term suggests an effect of cable installation. Comments explain patterns of results or propose possible factors influencing differences detected among treatments. ** = sig. ≤0.001 * = sig. <0.05, - indicates absent from region.

Taxon	SHELF			NECK			SLOPE			Comments
	P	T	PxT	P	T	PxT	P	T	PxT	
Higher taxa groups										
Multivariate Tests										
All Groups	*	ns	ns	ns	ns	ns	ns	*	ns	
Univariate Tests										
Actinaria (anemones)	ns	ns	ns	ns	ns	ns	ns	ns	ns	
Ceriantharia (tube anemones)	ns	ns	ns	ns	ns	ns	ns	ns	ns	
Pennatulacea (sea pens)	ns	ns	ns	ns	ns	ns	ns	*	ns	Cable > control at some stations
Asteroidea (sea stars)	*	ns	ns	ns	ns	ns	ns	ns	ns	Natural variability
Echinoidea (sea urchins)	-	-	-	ns	ns	ns	ns	ns	ns	
Holothuroidea (sea cucumbers)	ns	ns	ns	ns	ns	ns	*	*	*	Naturally variability One aggregation
Ophiuroidea (brittle stars)	*	ns	ns	ns	ns	ns	ns	ns	ns	Natural variability
Gastropoda (snails)	*	ns	ns	ns	ns	ns	ns	ns	ns	Natural variability
Pleuronectiformes (flatfishes)	ns	ns	ns	ns	*	ns	*	ns	ns	Control > Cable in all periods at Neck. Higher than normal numbers in 2010 at Slope control & cable stations
Sebastidae (rockfish)	ns	ns	ns	ns	ns	ns	**	ns	ns	Higher numbers in 2015 and 2020 at control & cable
Species										
Multivariate Tests										
All Species	*	ns	ns	ns	ns	ns	*	ns	ns	
Univariate Tests										
Funiculina sp. (sea pen)	-	-	-	-	-	-	ns	ns	ns	
Rathbunaster californicus (sea star)	ns	ns	ns	ns	ns	ns	ns	ns	ns	
Stronglylocentrotus fragilis (urchin)	-	-	-	ns	ns	ns	ns	ns	ns	
Psolus squamatus (sea cucumber)	-	-	-	ns	ns	ns	-	-	-	
Isoscyonis sp. (anemone)	-	-	-	-	-	-	ns	ns	ns	
Umbellula lindahli (sea pen)	-	-	-	-	-	-	*	ns	ns	Natural variability
Actinostolidae (anemone)	-	-	-	ns	ns	ns	*	ns	ns	Natural variability
Florometra serratissima (crinoid)	-	-	-	ns	ns	ns	-	-	-	
Pannychia moseleyi (sea cucumber)	-	-	-	-	-	-	*	*	*	Naturally variability One aggregation

Biological macrofauna assemblages

Regional effects of cable installation

Macrofaunal assemblages along the cable route appear to be largely unaffected by the installation and presence of the cable (Table 7–8, Fig. 16–18). Owing to the overwhelming dominance of polychaete worms in the macrofauna at the Shelf depth region (Table 7, Fig. 16), this group had a large influence on the outcome of our multivariate tests.

At Shelf, Neck and Slope regions, multivariate comparisons (i.e., comparisons between the entire megafaunal assemblage by group) indicated no overall significant PxT interaction terms (p = 0.20, 0.94, 0.99 respectively). Multivariate tests the taxonomic group level show a significant effect for period at the shelf region (Table 8, p = 0.001), meaning that there were changes over time unrelated to the cable, and a significant effect for both period and treatment at the Neck region (p = 0.017, 0.012).

In the Shelf region, the cable is buried to a meter deep in the sand, and there has been no visible evidence of detrital accumulation or seabed alteration beyond the first few weeks after cable installation. There were high densities of Ophiuroidea (brittle stars) in 2010 (Fig. 16), particularly at the control station. In 2015 there were higher densities of both amphipods and tanaids. Ephemeral events such as these suggest natural fluctuations. There were significantly more polychaetes after cable installation (P, p = 0.001), and more so on the cable transect (PxT, p = 0.035). The density of amphipods (P, p = 0.002), bivalves (P, p = 0.021), oligochaetes (P, p = 0.006), and ophiuroids (P, p = 0.002) also appear to have increased at both control and cable stations (Fig. 16). Given this, it is more likely that other factors (e.g., sample method difference in "before" samples, natural variability) had a greater influence on densities than any effect of the cable.

The density of bivalves was lower at the cable station (Fig. 17) in the Neck region where the cable is exposed, compared to Neck control stations. The bivalve species found here are small, delicate clams that could conceivably be disadvantaged by fine sediment winnowing in this hard substrate area (Fig. 7), or by abnormal abrasion. Mild disturbance near the cable may promote small density increases in oligochaetes and tanaids. The large pulse of amphipods sampled here just after cable installation (2008) may also be a sign of increased density due to disturbance, and perhaps the increased organic matter present (Fig. 8). The most abundant amphipod species were tube-dwellers and are known to increase in number when disturbance occurs. Tests showed that there was a period and treatment effect at the Neck region (P, p = 0.07; T, p = 0.012). There is evidence of a "before" sampling difference in the Neck region for polychaetes (P, p = 0.008) cable station as well, with initial numbers lower than the density variations seen in "after" samples (Fig. 17). There was a treatment effect for bivalves (p = 0.001), oligochaetes (p = 0.021) and tanaids (p = 0.004).

Some signs of disturbance in at the Slope cable station, which is at the MARS node site, were observed. Likely signs of disturbance in the form of physical displacement, changing grainsize (Fig. 7), and eutrophication (Fig. 8) included higher densities of oligochaetes (T, p = 0.011) and lower densities of bivalves (T, p = 0.029) and polychaete worms (P, p = 0.023). The Slope cable station is uniquely disturbed on a regular basis as the node is visited by ROV to set up and monitor the various experiments and equipment attached to the MARS node.

Together, these results indicate few detectable effects of the MARS cable on seabed biology, and are similar to results reported in other studies. Kogan et al., (2006) reported few detectable effects of the ATOC submarine cable on benthic faunal patterns. They noted that the major effect of the cable was on organisms that attached to it, especially anemones, and also reported erosion of the seabed by strumming of the exposed cable at shallow depths.

Table 7. Mean density of macrofaunal taxa, by group over all samples. Density is listed as number of individuals per core (volume = 187 cm^3), with the standard error of the mean (SE) and the percentage of total macrofaunal density.

Phylum	Group	Mean	SE	%
Annelida		**29.92**	**1.70**	**51.1**
	Polychaeta	26.71	1.28	45.6
	Oligochaeta	2.88	0.32	4.9
	Echiura	0.33	0.10	0.6
Arthropoda		**18.74**	**1.86**	**31.9**
	Amphipoda	11.26	0.86	19.2
	Tanaidacea	3.05	0.44	5.2
	Isopoda	1.50	0.16	2.6
	Ostracoda	1.47	0.23	2.5
	Cumacea	1.37	0.14	2.3
	Mysida	0.08	0.02	0.1
	Decapoda	0.01	0.01	0.0
Mollusca		**5.44**	**0.52**	**9.2**
	Bivalvia	3.93	0.30	6.7
	Gastropoda	0.91	0.12	1.5
	Scaphopoda	0.45	0.06	0.8
	Aplacophora	0.13	0.03	0.2
	Polyplacophora	0.02	0.01	0.0
Echinodermata		**2.44**	**0.40**	**4.2**
	Ophiuroidea	2.40	0.38	4.1
	Holothuroidea	0.03	0.01	0.1
	Echinoidea	0.01	0.01	0.0
Nemertea		**1.37**	**0.12**	**2.3**
Cnidaria		**0.37**	**0.08**	**0.7**
Platyhelminthes		**0.13**	**0.04**	**0.2**
Enteropneusta		**0.08**	**0.03**	**0.1**
Sipuncula		**0.07**	**0.02**	**0.1**
Phoronida		**0.03**	**0.01**	**0.1**
Total		**58.63**		

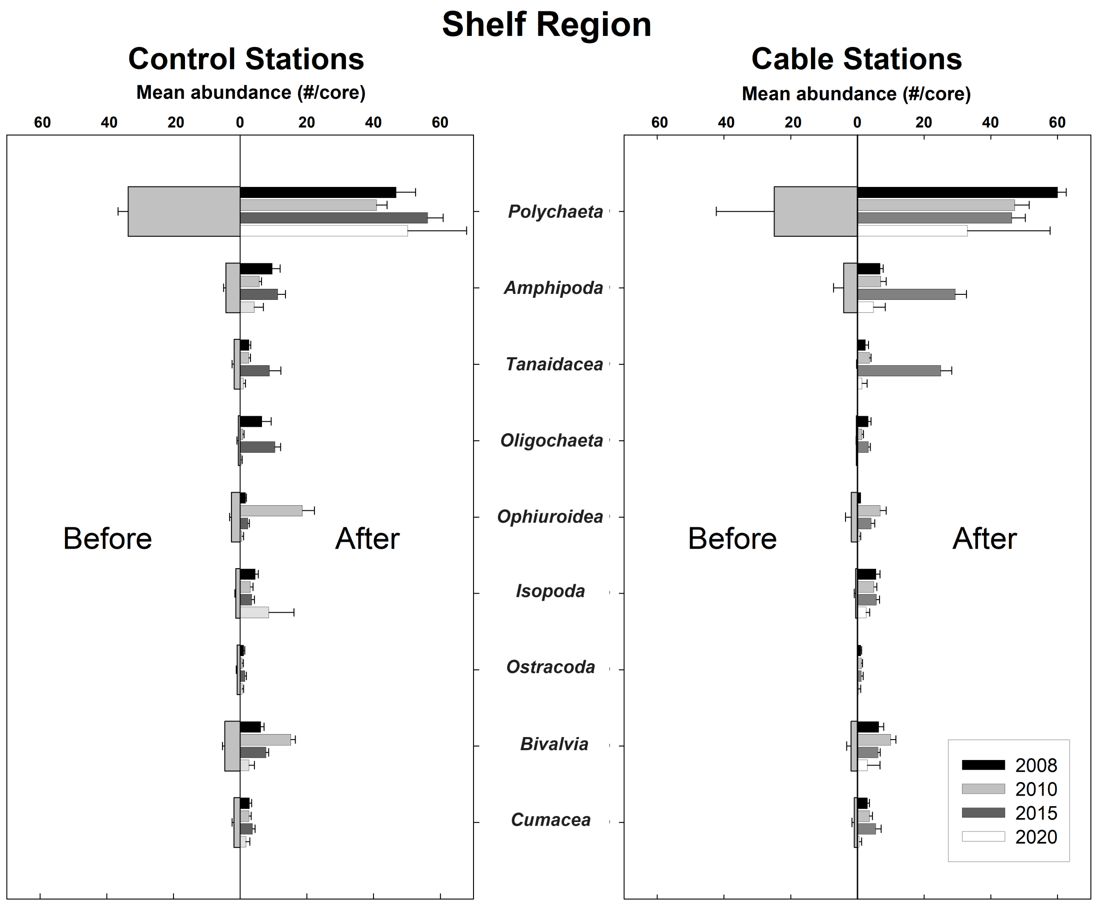

Figure 16. Variation in the abundance of major groups of macrofaunal taxa at the Shelf cable region among treatments and periods. The cable has been buried to 1 m depth here since installation, therefore differences in sampling technique before and after likely explain abundance differences in polychaete worms, amphipods and oligochaetes. A naturally occurring aggregation of brittlestars (Ophiuroidea) occurred in 2010. Error bars = standard error of the mean.

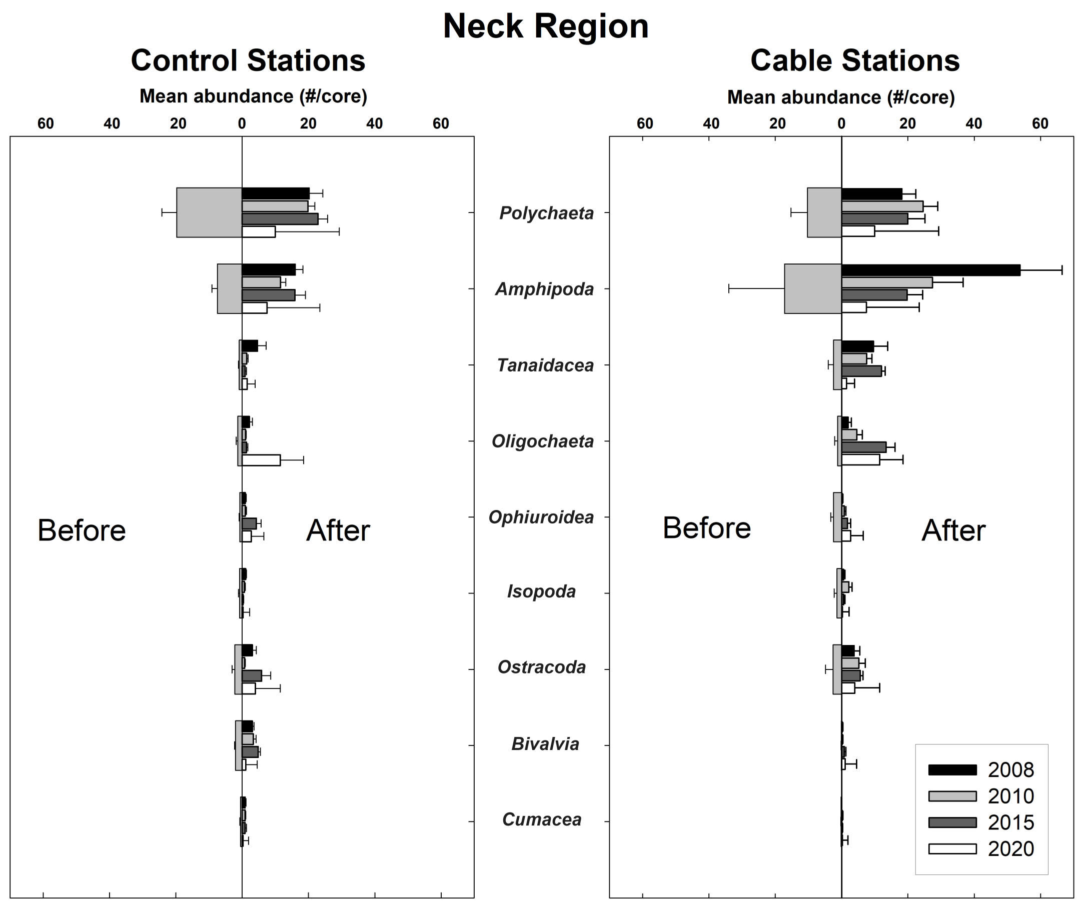

Figure 17. Variation in the abundance of major groups of macrofaunal taxa at the Neck cable region among treatments and periods. Polychaete worm abundance naturally varied at both control and cable stations over time. Higher abundance for tanaids and oligochaetes (2008–2015), and lower abundance for bivalves are likely due to disturbance at the cable station. Error bars = standard error of the mean.

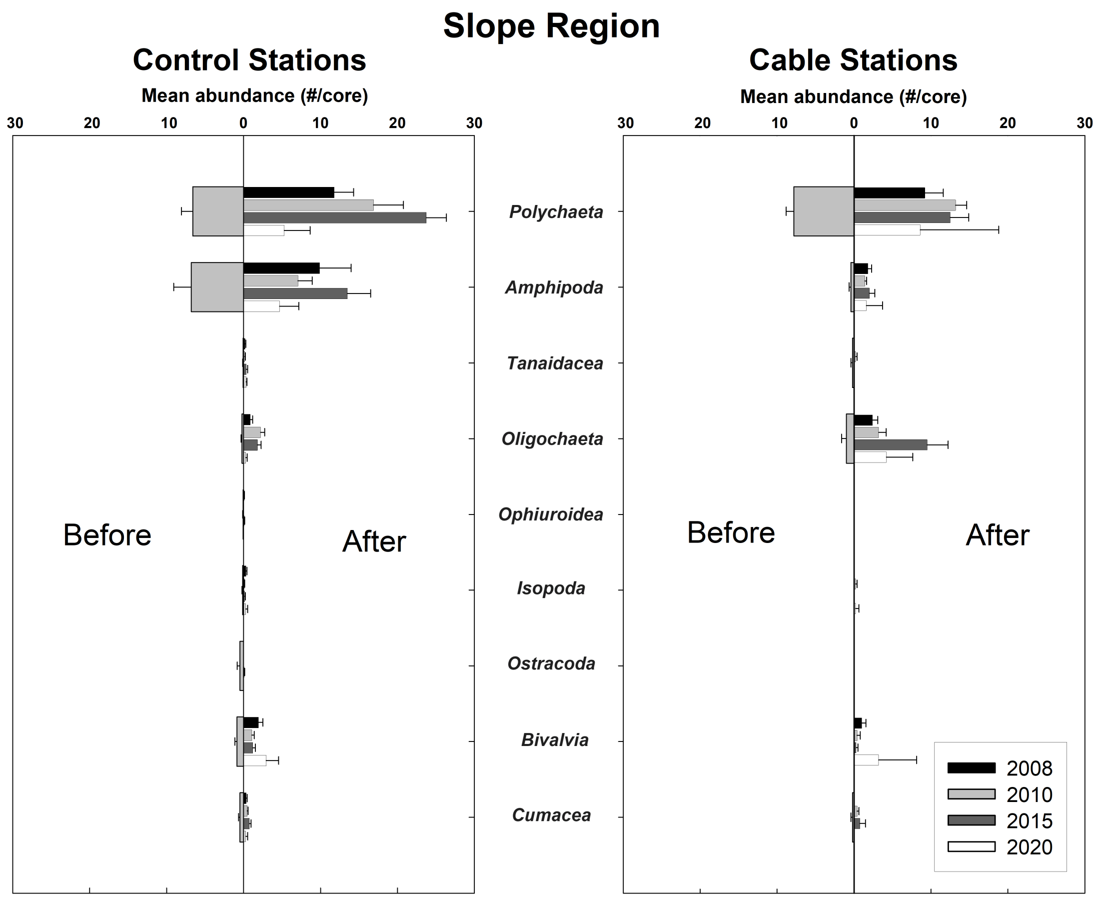

Figure 18. Variation in the abundance of major groups of macrofaunal taxa at the Slope cable region among treatments and periods. Polychaete worm abundance naturally varied at both control and cable stations over time. Treatment effects were seen for oligochaetes (higher abundance at the cable station), and bivalves (lower abundance at the cable station. Error bars = standard error of the mean.

Table 8. Summary of BACI analysis for macrofaunal taxa. P = Period, T= Treatment, PxT = Period x Treatment interaction term. A significant PxT term suggests an effect of cable installation. Comments explain patterns of results or propose possible factors influencing differences detected among treatments. * = $p < 0.05$, ** = $p \leq 0.001$.

Taxon	SHELF			NECK			SLOPE			Comments
	P	T	PxT	P	T	PxT	P	T	PxT	
Higher Taxa Groups										
Multivariate Tests										
All Groups	**	ns	ns	*	*	ns	ns	ns	ns	
Univariate Tests										
Polychaeta (worms)	**	ns	*	*	ns	ns	*	ns	ns	Sampling difference before vs. after at Shelf, nat. variability at Neck, Slope
Amphipoda (crustacea)	**	ns	ns	ns	ns	ns	ns	ns	ns	Sampling difference before vs. after at Shelf
Bivalvia (clams)	*	ns	ns	ns	**	ns	ns	*	ns	Sampling difference before vs. after at Shelf, lower density at cable in Neck and Slope regions from disturbance?
Oligochaeta (worms)	*	ns	ns	ns	*	ns	ns	*	ns	Sampling difference before vs. after at Shelf, higher density at cable for Neck and Slope regions from disturbance?
Tanaidacea (crustacea)	ns	ns	ns	ns	*	ns	ns	ns	ns	Higher density at cable in Neck region from disturbance?
Isopoda (crustacea)	ns	ns	ns	ns	ns	ns	ns	ns	ns	
Ostracoda (crustacea)	ns	ns	ns	ns	ns	ns	ns	ns	ns	
Ophiuroidea (brittle stars)	*	ns	ns	ns	ns	ns	ns	ns	ns	Aggregations, natural variation

Other factors influencing faunal patterns

Several other factors may have influenced the observed variability in the density and distribution of benthic megafauna and macrofauna in relation to the installation of the MARS Cable. First, the geological and biological sampling program included a few megafaunal transects collected as early as 1999 and 2001; these were included in the 'Before' transects collected principally during 2008. Therefore, estimates of megafaunal density during this extended 'Before' sampling period reflect, in part, the natural variability of local benthic communities. Subsequent samples were generally collected over shorter periods, and were more representative of a "snap shot" of benthic faunal communities for each sampling period.

Methods for sampling seabed sediments for macrofaunal analyses differed among sampling periods and are likely to have influenced the results (i.e., abundances of infaunal species collected). Samples collected prior to cable installation were collected in 1999 using a Smith-MacIntyre Grab (0.9 x 0.9 m). All subsequent sediment samples, including all post-installation samples, were taken using ROV-operated 6.9 cm diameter tube cores. The densities of macrofauna derived from Smith-MacIntyre grabs were adjusted by volume to match the volume of ROV push cores, but differences in the collection efficiency of the two devices is likely to have affected the results.

Uniquely, abundant biological detritus in the form of dead and dying pyrosomes, was present during the 2020 study period. No pyrosome detritus was observed on the seafloor during previous surveys. On the central coast, dead and dying pyrosomes were first seen by MBARI in increased numbers at a recurrently-sampled site (Station M, 4000 m, SW of the current study area) in the fall of 2012 (Kuhnz et al., 2020). They were rarely observed anywhere off central California prior to 2012 (Jacobsen Stout et al., 2020). At least 30 different taxa feed on these midwater tunicates; they are eaten by anemones, snails, sea stars, crinoids, sea cucumbers, urchins and crabs (Jacobsen Stout et al., 2020). This large flux of carbon to the seafloor could potentially alter biological community composition, at least over the short-term.

CONCLUSIONS

Inspection of the MARS cable, coupled with a sampling program to evaluate changes in surficial sediments and biological conditions on local and regional scales with respect to the installation of the cable indicate little detectable influence of the cable. The most conspicuous evidence of cable installation is the cable exposed on the seabed where it could not be buried. Analyses of the geological and biological sampling program indicate the following:

- Over most of its length, the cable remains buried, with little evidence of change since installation
- Changes in mean grain size were minor in relation to the MARS cable.
- The percent organic carbon content of sediments increased near the MARS cable at some depths, possibly due to natural variation or the effects of the cable or both.
- Local variation in benthic megafaunal communities within 50–100 m of the MARS cable is minor or undetectable.
    - The densities of most animals observed did not differ between the area over the cable route and 50 m away.
    - Longnose skates *(Bathyraja rhina*) were significantly more abundant in one area in 2008 where the MARS cable (unenergized at the time) was suspended over bathymetry (~300 m depth). These animals may have responded to weak electromagnetic fields surrounding the cable. After 2010, when the cable was energized, the numbers of *B. rhina* were near background levels near and distant from the cable.
- The MARS cable has little effect on the distribution and density of macrofaunal and megafaunal assemblages on a regional scale (e.g., kilometers).
    - Megafauna and macrofauna compared before and after cable installation among three control stations and one cable station at each of three depth regions (Shelf: <200 m, Neck: 200–500 m, Slope: >500 m) indicated relatively few potential changes in benthic biological patterns due to the MARS cable.
    - Natural spatial and temporal variation in the density and distribution of benthic macrofauna and megafauna is greater than any biological change associated with the installation of the MARS cable.

Video of the entire cable route has been copied to DVDs or hard drives and provided to agencies with each successive report.

ACKNOWLEDGEMENTS

This study was funded by the National Science Foundation (grants OCE-0222650, OCE-0739828) and the David and Lucille Packard Foundation. We are grateful for the expertise and support of the crews of the R/V *Point Lobos*, R/V *Rachel Carson*, ROV *Ventana*, ROV *Doc Ricketts*, and R/V *Western Flyer.* These activities were conducted under National Marine Sanctuary Permit MBNMS-2015-002 and MBNMS-2002-039.

REFERENCES

Barry, J.P., Kuhnz, L.A., Buck, K., Lovera, C., Whaling, P.J., 2007. MARS Post-Lay Inspection and Burial Report. Moss Landing, Califormia.

Bullock, T.H., 1982. Electroreception. Annu. Rev. Neurosci. 5, 121–170.

Cabin, R.J., Mitchell, R.J., 2000. To Bonferroni or Not to Bonferroni: When and How Are the Questions. Bull. Ecol. Soc. Am. 81, 246. doi:10.2307/20168454

Gill, A.B., 2005. Offshore renewable energy: Ecological implications of generating electricity in the coastal region. J. Appl. Ecol. 42, 605–615. doi:10.1111/j.1365-2664.2005.01060.x

Gill, A.B., Bartlett, M., Thomsen, F., 2012. Potential interactions between diadromous fishes of U.K. conservation importance and the electromagnetic fields and subsea noise from marine renewable energy developments. J. Fish Biol. 81, 664–695. doi:10.1111/j.1095-8649.2012.03374.x

Hewitt, J.E., Thrush, S.E., Cummings, V.J., 2001. Assessing Environmental Impacts: Effects Of Spatial And Temporal Variability At Likely Impact Scales. Ecol. Appl. 11, 1502–1516.

Howe, B.M., Arbic, B.K., Aucan, J., Barnes, C., Bayliff, N., Becker, N., Butler, R., Doyle, L., Elipot, S., Johnson, G.C., Landerer, F., Lentz, S., Luther, D.S., Müller, M., Mariano, J., Panayotou, K., Rowe, C., Scholl, R., Ota, H., Song, Y.T., Thomas, M., Thomas, P.N., Thompson, P., Tilmann, F., Weber, T., Weinstein, S., 2019. Smart cables for observing the global ocean: Science and implementation. Front. Mar. Sci. 6, 1–27. doi:10.3389/fmars.2019.00424

Jacobsen Stout, N., Kuhnz, L., Lundsten, B., Schlining, K., Barry, J.P., Kuhnz, L.A., Buck, K., Lovera, C., Whaling, P.J., 2007. MARS Post-Lay Inspection and Burial Report. Moss Landing, California.

Bullock, T.H., 1982. Electroreception. Annu. Rev. Neurosci. 5, 121–170.

Cabin, R.J., Mitchell, R.J., 2000. To Bonferroni or Not to Bonferroni: When and How Are the Questions. Bull. Ecol. Soc. Am. 81, 246. doi:10.2307/20168454

Gill, A.B., 2005. Offshore renewable energy: Ecological implications of generating electricity in the coastal region. J. Appl. Ecol. 42, 605–615. doi:10.1111/j.1365-2664.2005.01060.x

Gill, A.B., Bartlett, M., Thomsen, F., 2012. Potential interactions between diadromous fishes of U.K. conservation importance and the electromagnetic fields and subsea noise from marine renewable energy developments. J. Fish Biol. 81, 664–695. doi:10.1111/j.1095-8649.2012.03374.x

Hewitt, J.E., Thrush, S.E., Cummings, V.J., 2001. Assessing Environmental Impacts: Effects Of Spatial And Temporal Variability At Likely Impact Scales. Ecol. Appl. 11, 1502–1516.

Howe, B.M., Arbic, B.K., Aucan, J., Barnes, C., Bayliff, N., Becker, N., Butler, R., Doyle, L., Elipot, S., Johnson, G.C., Landerer, F., Lentz, S., Luther, D.S., Müller, M., Mariano, J., Panayotou, K., Rowe, C., Scholl, R., Ota, H., Song, Y.T., Thomas, M., Thomas, P.N., Thompson, P., Tilmann, F., Weber, T., Weinstein, S., 2019. Smart cables for observing the global ocean: Science and implementation. Front. Mar. Sci. 6, 1–27. doi:10.3389/fmars.2019.00424

Jacobsen Stout, N., Kuhnz, L., Lundsten, B., Schlining, K., Schlining, B., Von Thun, S. (Eds.), 2020. The Deep-Sea Guide (DSG). Monterey Bay Aquarium Research institute (MBARI).

Kogan, I., Paull, C.K., Kuhnz, L.A., Burton, E.J., Von Thun, S., Gary Greene, H., Barry, J.P., 2006. ATOC/Pioneer Seamount cable after 8 years on the seafloor: Observations, environmental impact. Cont. Shelf Res. 26, 771–787. doi:10.1016/j.csr.2006.01.010

Kuhnz, L.A., Ruhl, H.A., Huffard, C.L., Smith, K.L., 2020. Benthic megafauna assemblage change over three decades in the abyss: Variations from species to functional groups. Deep. Res. Part II Top. Stud. Oceanogr. 104761. doi:10.1016/j.dsr2.2020.104761

Love, M.S., Nishimoto, M.M., Clark, S., McCrea, M., Bull, A.S., 2017. The Organisms Living Around Energized Submarine Power Cables, Pipe, and Natural Sea Floor in the Inshore Waters of Southern California. Bull. South. Calif. Acad. Sci. 116, 61–87. doi:10.3160/soca-116-02-61-87.1

Martin Taylor, S., 2008. Transformative ocean science through the VENUS and NEPTUNE Canada ocean observing systems. Nucl. Instruments Methods Phys. Res. Sect. A Accel. Spectrometers, Detect. Assoc. Equip. 602, 63–67. doi:10.1016/j.nima.2008.12.019

Mikheev, V.N., Afonina, M.O., Pavlov, D.S., 2010. Habitat heterogeneity and fish behavior: Units of heterogeneity as a resource and as a source of information. J. Ichthyol. 50, 386–395. doi:10.1134/S0032945210050048

Normandeau, Exponent, Tricas, T., Gill, A., 2011. Effects Of EMF's From Undersea Power Cables On Elasmobranchs And Other Marine Species. U.S. Dept. of the Interior, Bureau of Ocean Energy Management, Regulation, and Enforcement, Pacific OCS Region, Camarillo, CA.

Perneger, T. V., 1998. What's wrong with Bonferroni adjustments. Br. Med. J. 316, 1236–1238. doi:10.1136/bmj.316.7139.1236

Schlining, B.M., Stout, N.J., 2006. MBARI's Video Annotation and Reference System, in: Proceedings of the Marine Technology Society/Institute of Electrical and Electronics Engineers Oceans Conference. pp. 1–5.

Slater, M., Schultz, A., Jones, R., Fischer, C., 2010. Electromagnetic Field Study.

Snoek, R., de Swart, R., Didderen, K., Lengkeek, W., Teunis, M., 2016. Potential effects of electromagnetic fields in the Dutch North Sea Phase 1 – Desk Study.
Stewart-Oaten, A., Murdoch, W.W., Parker, K.R., 1986. Environmental Impact Assessment: "Pseudoreplication" in Time? Ecology 67, 929–940. doi:10.1145/2482540.2482571

Suyehiro, K., Mikada, H., Asakawa, K., 2003. Japanese seafloor observing systems: Present and future. Mar. Technol. Soc. J. 37, 102–114. doi:10.4031/002533203787537230

Trowbridge, J., Weller, R., Kelley, D., Dever, E., Plueddemann, A., Barth, J.A., Kawka, O., 2019. The ocean observatories initiative. Front. Mar. Sci. 6, 1–23. doi:10.3389/fmars.2019.00074

Underwood, A.J., 1994. On Beyond BACI: Sampling Designs that Might Reliably Detect Environmental Disturbances. Ecol. Appl. 4, 3–15.

Appendix 1. ROV quantitative video transect information. Tr. Code = transect code, Loc. = Station.

Tr. Code	Loc.	Region	Treatment	Period	Latitude	Longitude	Depth (m)	Date	Dive #
A-A-2008	A	Slope	Cable	2008	36.756899	-122.188391	710	12/12/07	V3139
A-A-2010	A	Slope	Cable	2010	36.756645	-122.188324	720	1/27/10	V3500
A-A-2015	A	Slope	Cable	2015	36.756645	-122.188324	720	12/17/14	D703
A-A-2020	A	Slope	Cable	2020	36.755614	-122.187358	731	02/19/20	V4277
A-B-2008	A	Slope	Control	2008	36.756899	-122.187710	724	12/12/07	V3139
A-B-2010	A	Slope	Control	2010	36.757187	-122.187790	713	1/27/10	V3500
A-B-2015	A	Slope	Control	2015	36.757187	-122.187790	713	12/17/14	D703
A-B-2020	A	Slope	Control	2020	36.754729	-122.187788	743	02/19/20	V4277
B-A-2008	B	Slope	Cable	2008	36.799730	-122.186883	435	1/29/08	V3164
B-A-2010	B	Slope	Cable	2010	36.800182	-122.186560	431	1/29/10	V3506
B-A-2015	B	Slope	Cable	2015	36.800182	-122.186560	431	12/18/14	D705
B-A-2020	B	Slope	Cable	2020	36.799354	-122.187201	434	02/19/20	V4278
B-B-2008	B	Slope	Control	2008	36.799712	-122.186290	431	1/29/08	V3164
B-B-2010	B	Slope	Control	2010	36.799267	-122.186540	436	1/29/10	V3506
B-B-2015	B	Slope	Control	2015	36.799267	-122.186540	436	12/18/14	D705
B-B-2020	B	Slope	Control	2020	36.798225	-122.186975	437	02/19/20	V4278
C-A-2008	C	Neck	Cable	2008	36.836974	-122.158251	172	1/31/08	V3167
C-A-2010	C	Neck	Cable	2010	36.836964	-122.158460	168	1/13/10	V3488
C-A-2015	C	Neck	Cable	2015	36.836964	-122.158460	168	12/18/15	V3893
C-A-2020	C	Neck	Cable	2020	36.835281	-122.160528	217	01/14/20	V4256
C-B-2008	C	Neck	Control	2008	36.837340	-122.158864	162	1/31/08	V3167
C-B-2010	C	Neck	Control	2010	36.836964	-122.157170	153	1/13/10	V3488
C-B-2015	C	Neck	Control	2015	36.836964	-122.157170	153	12/18/15	V3893
C-B-2020	C	Neck	Control	2020	36.836655	-122.159726	189	01/14/20	V4256
D-A-2008	D	Shelf	Cable	2008	36.857358	-122.108810	95	2/8/08	V3169
D-A-2010	D	Shelf	Cable	2010	36.857227	-122.109116	92	1/28/10	V3503
D-A-2015	D	Shelf	Cable	2015	36.857227	-122.109116	92	7/9/15	V3842
D-B-2008	D	Shelf	Control	2008	36.856905	-122.108491	94	2/8/08	V3169
D-B-2010	D	Shelf	Control	2010	36.857254	-122.107834	92	1/28/10	V3503
D-B-2015	D	Shelf	Control	2015	36.857254	-122.107834	92	7/9/15	V3842
E-A-2008	E	Shelf	Cable	2008	36.879787	-122.059782	72	4/1/08	V3186
E-A-2010	E	Shelf	Cable	2010	36.879307	-122.061250	73	2/25/10	V3526
E-A-2015	E	Shelf	Cable	2015	36.879307	-122.061250	73	12/18/15	V3895
E-A-2020	E	Shelf	Cable	2020	36.879985	-122.059693	70	11/20/19	V4237
E-B-2008	E	Shelf	Control	2008	36.880117	-122.060248	71	4/1/08	V3186
E-B-2010	E	Shelf	Control	2010	36.880060	-122.060875	72	2/25/10	V3526
E-B-2015	E	Shelf	Control	2015	36.880060	-122.060875	72	12/18/15	V3895
E-B-2020	E	Shelf	Control	2020	36.879607	-122.05828	69	11/20/19	V4237
F-A-2008	F	Shelf	Cable	2008	36.885715	-122.006020	48	4/1/08	V3186
F-A-2010	F	Shelf	Cable	2010	36.885746	-122.005420	48	4/9/10	V3551
F-A-2015	F	Shelf	Cable	2015	36.885746	-122.005420	48	7/14/15	V3844
F-A-2020	F	Shelf	Cable	2020	36.885712	-122.00516	45	02/05/20	V4270
F-B-2008	F	Shelf	Control	2008	36.885231	-122.006393	49	4/1/08	V3186
F-B-2010	F	Shelf	Control	2010	36.886240	-122.006610	48	4/9/10	V3551
F-B-2015	F	Shelf	Control	2015	36.886240	-122.006610	48	7/14/15	V3844
F-B-2020	F	Shelf	Control	2020	36.88509	-122.001604	44	02/05/20	V4270
G-A-2008	G	Shelf	Cable	2008	36.883813	-121.949321	39	1/8/08	V3149
G-A-2010	G	Shelf	Cable	2010	36.883705	-121.949730	39	4/9/10	V3552
G-A-2015	G	Shelf	Cable	2015	36.883705	-121.949730	39	7/14/15	V3845
G-A-2020	G	Shelf	Cable	2020	36.88366	-121.949676	37	11/19/19	V4235
G-B-2008	G	Shelf	Control	2008	36.883895	-121.949741	40	1/8/08	V3149
G-B-2010	G	Shelf	Control	2010	36.884678	-121.950645	37	4/9/10	V3552
G-B-2015	G	Shelf	Control	2015	36.884678	-121.950645	37	7/14/15	V3845
G-B-2020	G	Shelf	Control	2020	36.882682	-121.948531	38	11/19/19	V4235

Tr. Code	Loc.	Region	Treatment	Period	Latitude	Longitude	Depth (m)	Date	Dive #
H-A-2008	H	Shelf	Cable	2008	36.868305	-121.895886	44	1/28/08	V3163
H-A-2010	H	Shelf	Cable	2010	36.868030	-121.896835	46	4/9/10	V3553
H-A-2015	H	Shelf	Cable	2015	36.868030	-121.896835	46	7/14/15	V3845
H-A-2020	H	Shelf	Cable	2020	36.868245	-121.897742	43	12/05/19	V4246
H-B-2008	H	Shelf	Control	2008	36.867867	-121.896324	44	1/28/08	V3163
H-B-2010	H	Shelf	Control	2010	36.868860	-121.897860	44	4/9/10	V3553
H-B-2015	H	Shelf	Control	2015	36.868860	-121.897860	44	7/14/15	V3845
H-B-2020	H	Shelf	Control	2020	36.867322	-121.896613	43	12/05/19	V4246
I-A-2008	I	Shelf	Cable	2008	36.848015	-121.845586	26	1/22/10	V3173
I-A-2010	I	Shelf	Cable	2010	36.848717	-121.847100	26	4/9/10	V3554
I-A-2015	I	Shelf	Cable	2015	36.848717	-121.847100	26	7/15/15	V3846
I-B-2008	I	Shelf	Control	2008	36.847485	-121.844780	26	1/22/10	V3173
I-B-2010	I	Shelf	Control	2010	36.849445	-121.847560	26	4/9/10	V3554
I-B-2015	I	Shelf	Control	2015	36.849445	-121.847560	26	7/15/15	V3846
J-A-2008	J	Shelf	Cable	2008	36.815585	-121.807344	20	3/31/08	V3184
J-A-2010	J	Shelf	Cable	2010	36.816120	-121.807730	20	4/9/10	V3555
J-A-2015	J	Shelf	Cable	2015	36.816120	-121.807730	20	7/15/15	V3846
J-B-2008	J	Shelf	Control	2008	36.816038	-121.806923	20	3/31/08	V3184
J-B-2010	J	Shelf	Control	2010	36.817257	-121.808020	19	4/9/10	V3555
J-B-2015	J	Shelf	Control	2015	36.817257	-121.808020	19	7/15/15	V3846
NC1-A-2005	NC-1	Neck	Control	Before	36.789158	-122.124280	401	7/13/05	V2687
NC1-A-2008	NC-1	Neck	Control	2008	36.788543	-122.117341	399	1/30/08	V3165
NC1-A-2010	NC-1	Neck	Control	2010	36.788597	-122.116370	402	1/8/10	V3483
NC1-A-2015	NC-1	Neck	Control	2015	36.788597	-122.116370	402	12/19/14	D706
NC1-B-2005	NC-1	Neck	Control	Before	36.789383	-122.125140	400	7/13/05	V2687
NC1-B-2008	NC-1	Neck	Control	2008	36.789039	-122.117852	394	1/30/08	V3165
NC1-B-2010	NC-1	Neck	Control	2010	36.788810	-122.115770	401	1/8/10	V3483
NC1-B-2015	NC-1	Neck	Control	2015	36.788810	-122.115770	401	12/19/14	D706
NC1-C-2005	NC-1	Neck	Control	Before	36.788088	-122.121619	400	7/13/05	V2687
NC1-C-2008	NC-1	Neck	Control	2008	36.789491	-122.116151	386	1/30/08	V3165
NC1-C-2010	NC-1	Neck	Control	2010	36.789043	-122.116936	392	1/8/10	V3483
NC1-C-2015	NC-1	Neck	Control	2015	36.789043	-122.116936	392	12/19/14	D706
NC2-A-2005	NC-2	Neck	Control	Before	36.803011	-122.122515	196	8/1/05	V2696
NC2-A-2008	NC-2	Neck	Control	2008	36.799381	-122.107564	207	1/30/08	V3165
NC2-A-2010	NC-2	Neck	Control	2010	36.798930	-122.107700	205	1/8/10	V3483
NC2-A-2015	NC-2	Neck	Control	2015	36.798930	-122.107700	205	12/16/14	D701
NC2-B-2005	NC-2	Neck	Control	Before	36.803356	-122.123501	197	8/1/05	V2696
NC2-B-2008	NC-2	Neck	Control	2008	36.799928	-122.108486	189	1/30/08	V3165
NC2-B-2010	NC-2	Neck	Control	2010	36.798664	-122.106720	208	1/8/10	V3483
NC2-B-2015	NC-2	Neck	Control	2015	36.798664	-122.106720	208	12/16/14	D701
NC2-C-2005	NC-2	Neck	Control	Before	36.803646	-122.124485	198	8/1/05	V2696
NC2-C-2008	NC-2	Neck	Control	2008	36.799216	-122.108455	195	1/30/08	V3165
NC2-C-2010	NC-2	Neck	Control	2010	36.798023	-122.107780	222	1/8/10	V3483
NC2-C-2015	NC-2	Neck	Control	2015	36.798023	-122.107780	222	12/16/14	D701
NC3-A-2006	NC-3	Neck	Control	Before	36.842645	-122.189108	361	10/3/06	V2899
NC3-A-2008	NC-3	Neck	Control	2008	36.842894	-122.187867	361	1/24/08	V3162
NC3-A-2010	NC-3	Neck	Control	2010	36.842316	-122.187260	358	1/14/10	V3490
NC3-A-2015	NC-3	Neck	Control	2015	36.842316	-122.187260	358	12/19/14	D707
NC3-B-2006	NC-3	Neck	Control	Before	36.842120	-122.189979	368	10/3/06	V2899
NC3-B-2008	NC-3	Neck	Control	2008	36.842918	-122.187669	352	1/24/08	V3162
NC3-B-2010	NC-3	Neck	Control	2010	36.841690	-122.186264	360	1/14/10	V3490
NC3-B-2015	NC-3	Neck	Control	2015	36.841690	-122.186264	360	12/19/14	D707
NC3-C-2008	NC-3	Neck	Control	2008	36.842812	-122.186766	356	1/24/08	V3162
NC3-C-2010	NC-3	Neck	Control	2010	36.842228	-122.185660	349	1/14/10	V3490
NC3-C-2015	NC-3	Neck	Control	2015	36.842228	-122.185660	349	12/19/14	D707

Tr. Code	Loc.	Region	Treatment	Period	Latitude	Longitude	Depth (m)	Date	Dive #
NC1-A-2020	NC1	Neck	Control	2020	36.788725	-122.11648	398	12/05/19	V4244
NC1-B-2020	NC1	Neck	Control	2020	36.789665	-122.115753	385	12/05/19	V4244
NC1-C-2020	NC1	Neck	Control	2020	36.790172	-122.116898	376	12/05/19	V4244
NC2-A-2020	NC2	Neck	Control	2020	36.798545	-122.108343	212	12/05/19	V4244
NC2-B-2020	NC2	Neck	Control	2020	36.79872	-122.106928	205	12/05/19	V4244
NC2-C-2020	NC2	Neck	Control	2020	36.799622	-122.105777	193	12/05/19	V4244
NC3-A-2020	NC3	Neck	Control	2020	36.843972	-122.18685	333	01/14/20	V4255
NC3-B-2020	NC3	Neck	Control	2020	36.84325	-122.185937	332	01/14/20	V4255
NC3-C-2020	NC3	Neck	Control	2020	36.843089	-122.187415	349	01/14/20	V4255
NI1-A-1999	NI-1	Neck	Cable	Before	36.824453	-122.169606	325	1999	MCI-Pref325
NI1-A-2008	NI-1	Neck	Cable	2008	36.824453	-122.169606	321	1/31/08	V3167
NI1-A-2010	NI-1	Neck	Cable	2010	36.824330	-122.170204	323	1/13/10	V3488
NI1-A-2015	NI-1	Neck	Cable	2015	36.824330	-122.170204	323	12/19/14	D708
NI1-B-1999	NI-1	Neck	Cable	Before	36.824886	-122.170095	325	1999	MCI-Pref325
NI1-B-2008	NI-1	Neck	Cable	2008	36.824886	-122.170095	318	1/31/08	V3167
NI1-B-2010	NI-1	Neck	Cable	2010	36.823880	-122.170080	324	1/13/10	V3488
NI1-B-2015	NI-1	Neck	Cable	2015	36.823880	-122.170080	324	12/19/14	D708
NI1-C-1999	NI-1	Neck	Cable	Before	36.824287	-122.170539	325	1999	MCI-ACA325
NI1-C-2008	NI-1	Neck	Cable	2008	36.824287	-122.170539	323	1/31/08	V3167
NI1-C-2010	NI-1	Neck	Cable	2010	36.824795	-122.169190	321	1/13/10	V3488
NI1-A-2020	NI1	Neck	Cable	2020	36.82426	-122.169913	320	01/14/20	V4256
NI1-B-2020	NI1	Neck	Cable	2020	36.825806	-122.169482	315	01/14/20	V4256
NI1-C-2020	NI1	Neck	Cable	2020	36.825879	-122.170953	320	01/14/20	V4256
SC1-A-2006	SC-1	Shelf	Control	Before	36.714458	-121.909033	90	9/25/06	V2891
SC1-A-2008	SC-1	Shelf	Control	2008	36.714458	-121.909033	89	11/30/07	V3135
SC1-A-2010	SC-1	Shelf	Control	2010	36.715485	-121.908630	88	2/18/10	V3518
SC1-A-2015	SC-1	Shelf	Control	2015	36.715485	-121.908630	88	9/1/14	V3797
SC1-B-2006	SC-1	Shelf	Control	Before	36.714299	-121.908597	90	9/25/06	V2891
SC1-B-2008	SC-1	Shelf	Control	2008	36.714299	-121.908597	90	11/30/07	V3135
SC1-B-2010	SC-1	Shelf	Control	2010	36.714436	-121.908620	88	2/18/10	V3518
SC1-B-2015	SC-1	Shelf	Control	2015	36.714436	-121.908620	88	9/1/14	V3797
SC1-C-2006	SC-1	Shelf	Control	Before	36.713548	-121.907717	90	9/25/06	V2891
SC1-C-2008	SC-1	Shelf	Control	2008	36.713548	-121.907717	89	11/30/07	V3135
SC1-C-2010	SC-1	Shelf	Control	2010	36.714790	-121.907380	88	2/18/10	V3518
SC1-C-2015	SC-1	Shelf	Control	2015	36.714790	-121.907380	88	9/1/14	V3797
SC2-A-2006	SC-2	Shelf	Control	Before	36.821804	-121.944500	87	10/5/06	V2905
SC2-A-2008	SC-2	Shelf	Control	2008	36.822428	-121.945564	87	11/30/07	V3134
SC2-A-2010	SC-2	Shelf	Control	2010	36.821888	-121.945530	88	1/29/10	V3504
SC2-A-2015	SC-2	Shelf	Control	2015	36.821888	-121.945530	88	9/18/14	V3801
SC2-B-2006	SC-2	Shelf	Control	Before	36.822571	-121.943540	86	10/5/06	V2905
SC2-B-2008	SC-2	Shelf	Control	2008	36.822978	-121.944894	86	11/30/07	V3134
SC2-B-2010	SC-2	Shelf	Control	2010	36.822903	-121.945540	87	1/29/10	V3504
SC2-B-2015	SC-2	Shelf	Control	2015	36.822903	-121.945540	87	9/18/14	V3801
SC2-C-2008	SC-2	Shelf	Control	2008	36.823517	-121.944924	86	11/30/07	V3134
SC2-C-2010	SC-2	Shelf	Control	2010	36.823350	-121.946236	88	1/29/10	V3504
SC2-C-2015	SC-2	Shelf	Control	2015	36.823350	-121.946236	88	9/18/14	V3801
SC3-A-2006	SC-3	Shelf	Control	Before	36.878461	-122.121178	89	10/5/06	V2904
SC3-A-2008	SC-3	Shelf	Control	2008	36.877177	-122.120826	90	1/30/08	V3166
SC3-A-2010	SC-3	Shelf	Control	2010	36.878260	-122.121230	90	1/28/10	V3502
SC3-A-2015	SC-3	Shelf	Control	2015	36.878260	-122.121230	90	9/1/14	V3800
SC3-B-2006	SC-3	Shelf	Control	Before	36.878765	-122.120205	89	10/5/06	V2904
SC3-B-2008	SC-3	Shelf	Control	2008	36.877639	-122.121503	91	1/30/08	V3166
SC3-B-2010	SC-3	Shelf	Control	2010	36.878094	-122.119900	90	1/28/10	V3502
SC3-B-2015	SC-3	Shelf	Control	2015	36.878094	-122.119900	90	9/1/14	V3800
SC3-C-2008	SC-3	Shelf	Control	2008	36.877494	-122.120593	91	1/30/08	V3166

Tr. Code	Loc.	Region	Treatment	Period	Latitude	Longitude	Depth (m)	Date	Dive #
SC3-C-2010	SC-3	Shelf	Control	2010	36.876762	-122.119804	90	1/28/10	V3502
SC3-C-2015	SC-3	Shelf	Control	2015	36.876762	-122.119804	90	9/1/14	V3800
SC1-A-2020	SC1	Shelf	Control	2020	36.715179	-121.90793	88	02/05/20	V4268
SC1-B-2020	SC1	Shelf	Control	2020	36.714452	-121.909265	88	02/05/20	V4268
SC1-C-2020	SC1	Shelf	Control	2020	36.714555	-121.907604	87	02/05/20	V4268
SC2-A-2020	SC2	Shelf	Control	2020	36.822317	-121.945598	86	02/05/20	V4269
SC2-B-2020	SC2	Shelf	Control	2020	36.821686	-121.944498	85	02/05/20	V4269
SC2-C-2020	SC2	Shelf	Control	2020	36.821088	-121.945593	85	02/05/20	V4269
SC3-A-2020	SC3	Shelf	Control	2020	36.877603	-122.118742	88	11/20/19	V4236
SC3-B-2020	SC3	Shelf	Control	2020	36.87865	-122.118052	88	11/20/19	V4236
SC3-C-2020	SC3	Shelf	Control	2020	36.878083	-122.122632	88	11/20/19	V4236
SI1-A-1999	SI-1	Shelf	Cable	Before	36.863391	-122.096900	90	1999	MCI-ACAD90
SI1-A-2008	SI-1	Shelf	Cable	2008	36.863391	-122.096900	91	1/23/08	V3161
SI1-A-2010	SI-1	Shelf	Cable	2010	36.863014	-122.096540	89	1/28/10	V3503
SI1-A-2015	SI-1	Shelf	Cable	2015	36.863014	-122.096540	89	9/18/14	V3802
SI1-A-2020	SI-1	Shelf	Cable	2020	36.863093	-122.096575	88	11/20/19	V4237
SI1-B-1999	SI-1	Shelf	Cable	Before	36.863186	-122.096707	90	1999	MCI-ACAD90
SI1-B-2008	SI-1	Shelf	Cable	2008	36.863186	-122.096707	92	1/23/08	V3161
SI1-B-2010	SI-1	Shelf	Cable	2010	36.862130	-122.096330	89	1/28/10	V3503
SI1-B-2015	SI-1	Shelf	Cable	2015	36.862130	-122.096330	89	9/18/14	V3802
SI1-B-2020	SI-1	Shelf	Cable	2020	36.862792	-122.098302	89	11/20/19	V4237
SI1-C-2008	SI-1	Shelf	Cable	2008	36.863471	-122.096143	92	1/23/08	V3161
SI1-C-2010	SI-1	Shelf	Cable	2010	36.862755	-122.094860	89	1/28/10	V3503
SI1-C-2015	SI-1	Shelf	Cable	2015	36.862755	-122.094860	89	9/18/14	V3802
SI1-C-2020	SI-1	Shelf	Cable	2020	36.865127	-122.096753	88	11/20/19	V4237
Skate1-A-2008	Skate	Neck	Control	2008	36.825740	-122.168653	313	1/31/08	V3167
Skate1-A-2010	Skate	Neck	Control	2010	36.825740	-122.168653	313	1/13/10	V3488
Skate1-B-2008	Skate	Neck	Control	2008	36.826303	-122.168202	310	1/31/08	V3167
Skate1-B-2010	Skate	Neck	Control	2010	36.826303	-122.168202	310	1/13/10	V3488
Skate1-C-2008	Skate	Neck	Control	2008	36.827346	-122.167738	309	1/31/08	V3167
Skate1-C-2010	Skate	Neck	Control	2010	36.827346	-122.167738	309	1/13/10	V3488
Skate2-A-2008	Skate	Neck	Cable	2008	36.826029	-122.169319	317	1/31/08	V3167
Skate2-A-2010	Skate	Neck	Cable	2010	36.826029	-122.169319	317	1/13/10	V3488
Skate2-B-2008	Skate	Neck	Cable	2008	36.826903	-122.168852	311	1/31/08	V3167
Skate2-B-2010	Skate	Neck	Cable	2010	36.826903	-122.168852	311	1/13/10	V3488
Skate2-C-2008	Skate	Neck	Cable	2008	36.827570	-122.168474	306	1/31/08	V3167
Skate2-C-2010	Skate	Neck	Cable	2010	36.827570	-122.168474	306	1/13/10	V3488
SLC1-A-2001	SLC-1	Slope	Control	Before	36.743379	-122.275459	1000	10/12/01	V2083
SLC1-A-2008	SLC-1	Slope	Control	2008	36.745790	-122.277049	992	1/7/08	V3147
SLC1-A-2010	SLC-1	Slope	Control	2010	36.744267	-122.277030	1001	3/8/10	D115
SLC1-A-2015	SLC-1	Slope	Control	2015	36.744267	-122.277030	1001	12/17/14	D702
SLC1-B-2001	SLC-1	Slope	Control	Before	36.742199	-122.274547	1000	10/12/01	V2083
SLC1-B-2008	SLC-1	Slope	Control	2008	36.745207	-122.277572	1001	1/7/08	V3147
SLC1-B-2010	SLC-1	Slope	Control	2010	36.745200	-122.277725	1002	3/8/10	D115
SLC1-B-2015	SLC-1	Slope	Control	2015	36.745200	-122.277725	1002	12/17/14	D702
SLC1-C-2001	SLC-1	Slope	Control	Before	36.741165	-122.273010	999	10/12/01	V2083
SLC1-C-2008	SLC-1	Slope	Control	2008	36.745351	-122.278318	1007	1/7/08	V3147
SLC1-C-2010	SLC-1	Slope	Control	2010	36.744420	-122.278070	1006	3/8/10	D115
SLC1-C-2015	SLC-1	Slope	Control	2015	36.744420	-122.278070	1006	12/17/14	D702
SLC2-A-2005	SLC-2	Slope	Control	Before	36.752527	-122.200020	801	6/8/05	V2674
SLC2-A-2008	SLC-2	Slope	Control	2008	36.748745	-122.197382	820	1/23/08	V3160
SLC2-A-2010	SLC-2	Slope	Control	2010	36.749023	-122.197830	821	1/27/10	V3500
SLC2-A-2015	SLC-2	Slope	Control	2015	36.749023	-122.197830	821	12/18/14	D705
SLC2-B-2005	SLC-2	Slope	Control	Before	36.752640	-122.200906	800	6/8/05	V2674
SLC2-B-2008	SLC-2	Slope	Control	2008	36.748580	-122.197578	817	1/23/08	V3160

Tr. Code	Loc.	Region	Treatment	Period	Latitude	Longitude	Depth (m)	Date	Dive #
SLC2-B-2010	SLC-2	Slope	Control	2010	36.748340	-122.197580	820	1/27/10	V3500
SLC2-B-2015	SLC-2	Slope	Control	2015	36.748340	-122.197580	820	12/18/14	D705
SLC2-C-2005	SLC-2	Slope	Control	Before	36.752558	-122.202336	801	6/8/05	V2674
SLC2-C-2008	SLC-2	Slope	Control	2008	36.748988	-122.198433	827	1/23/08	V3160
SLC2-C-2010	SLC-2	Slope	Control	2010	36.749180	-122.196240	813	1/27/10	V3500
SLC2-C-2015	SLC-2	Slope	Control	2015	36.749180	-122.196240	813	12/18/14	D705
SLC3-A-2006	SLC-3	Slope	Control	Before	36.707094	-122.167266	881	10/3/06	V2898
SLC3-A-2008	SLC-3	Slope	Control	2008	36.705268	-122.166423	895	1/8/08	V3148
SLC3-A-2010	SLC-3	Slope	Control	2010	36.706226	-122.166200	885	3/9/10	D116
SLC3-A-2015	SLC-3	Slope	Control	2015	36.706226	-122.166200	885	12/18/14	D704
SLC3-B-2006	SLC-3	Slope	Control	Before	36.707753	-122.166954	877	10/3/06	V2898
SLC3-B-2008	SLC-3	Slope	Control	2008	36.706463	-122.165729	884	1/8/08	V3148
SLC3-B-2010	SLC-3	Slope	Control	2010	36.705530	-122.166090	892	3/9/10	D116
SLC3-B-2015	SLC-3	Slope	Control	2015	36.705530	-122.166090	892	12/18/14	D704
SLC3-C-2006	SLC-3	Slope	Control	Before	36.707710	-122.165860	874	10/3/06	V2898
SLC3-C-2008	SLC-3	Slope	Control	2008	36.705928	-122.164967	887	1/8/08	V3148
SLC3-C-2010	SLC-3	Slope	Control	2010	36.706146	-122.167200	885	3/9/10	D116
SLC3-C-2015	SLC-3	Slope	Control	2015	36.706146	-122.167200	885	12/18/14	D704
SLC1-A-2020	SLC1	Slope	Control	2020	36.745052	-122.278898	1008	12/03/19	V4241
SLC1-B-2020	SLC1	Slope	Control	2020	36.744412	-122.278035	1006	12/03/19	V4241
SLC1-C-2020	SLC1	Slope	Control	2020	36.744005	-122.278703	1012	12/03/19	V4241
SLC2-A-2020	SLC2	Slope	Control	2020	36.749838	-122.197366	815	01/30/20	V4266
SLC2-B-2020	SLC2	Slope	Control	2020	36.749531	-122.198068	819	01/30/20	V4266
SLC2-C-2020	SLC2	Slope	Control	2020	36.750121	-122.197417	815	01/30/20	V4266
SLC3-A-2020	SLC3	Slope	Control	2020	36.706727	-122.165718	882	12/04/19	V4242
SLC3-B-2020	SLC3	Slope	Control	2020	36.707827	-122.166092	874	12/04/19	V4242
SLC3-C-2020	SLC3	Slope	Control	2020	36.706997	-122.165073	882	12/04/19	V4242
SLI1-A-2003	SLI-1	Slope	Cable	Before	36.711241	-122.186781	885	10/13/03	V2439
SLI1-A-2008	SLI-1	Slope	Cable	2008	36.712528	-122.187070	877	12/6/07	V3136
SLI1-A-2010	SLI-1	Slope	Cable	2010	36.712750	-122.187164	877	3/8/10	D114
SLI1-A-2015	SLI-1	Slope	Cable	2015	36.712750	-122.187164	877	12/17/14	D703
SLI1-A-2020	SLI-1	Slope	Cable	2020	36.712451	-122.186923	878	01/30/20	V4267
SLI1-B-2003	SLI-1	Slope	Cable	Before	36.711353	-122.186449	883	10/13/03	V2439
SLI1-B-2008	SLI-1	Slope	Cable	2008	36.713020	-122.186753	877	12/6/07	V3136
SLI1-B-2010	SLI-1	Slope	Cable	2010	36.713116	-122.186900	875	3/8/10	D114
SLI1-B-2015	SLI-1	Slope	Cable	2015	36.713116	-122.186900	875	12/17/14	D703
SLI1-B-2020	SLI-1	Slope	Cable	2020	36.712811	-122.188072	880	01/30/20	V4267
SLI1-C-2003	SLI-1	Slope	Cable	Before	36.711883	-122.186523	882	10/13/03	V2439
SLI1-C-2008	SLI-1	Slope	Cable	2008	36.712683	-122.186665	874	12/6/07	V3136
SLI1-C-2010	SLI-1	Slope	Cable	2010	36.712590	-122.186890	877	3/8/10	D114
SLI1-C-2015	SLI-1	Slope	Cable	2015	36.712590	-122.186890	877	12/17/14	D703
SLI1-C-2020	SLI-1	Slope	Cable	2020	36.713534	-122.187855	875	01/30/20	V4267

Appendix 2. Condition of the MARS Cable and surficial habitat disturbance.

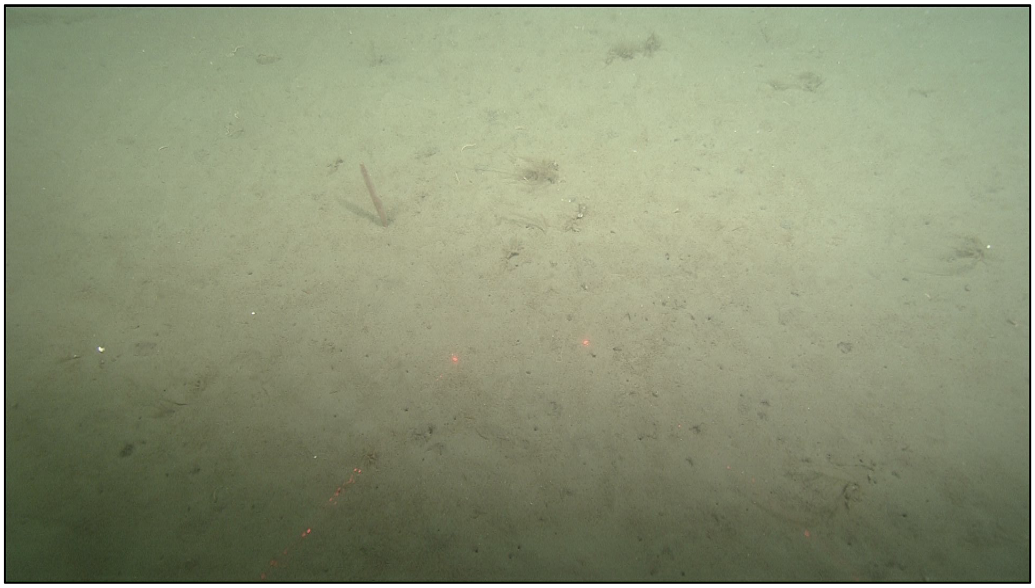

Figure A. In shallow regions (0–115 m depth), the cable has been buried in sand since 2007 with no trace of the cable, cable trench or other disturbance for the first 34.45 km of the route. This image is from 28 m in depth.

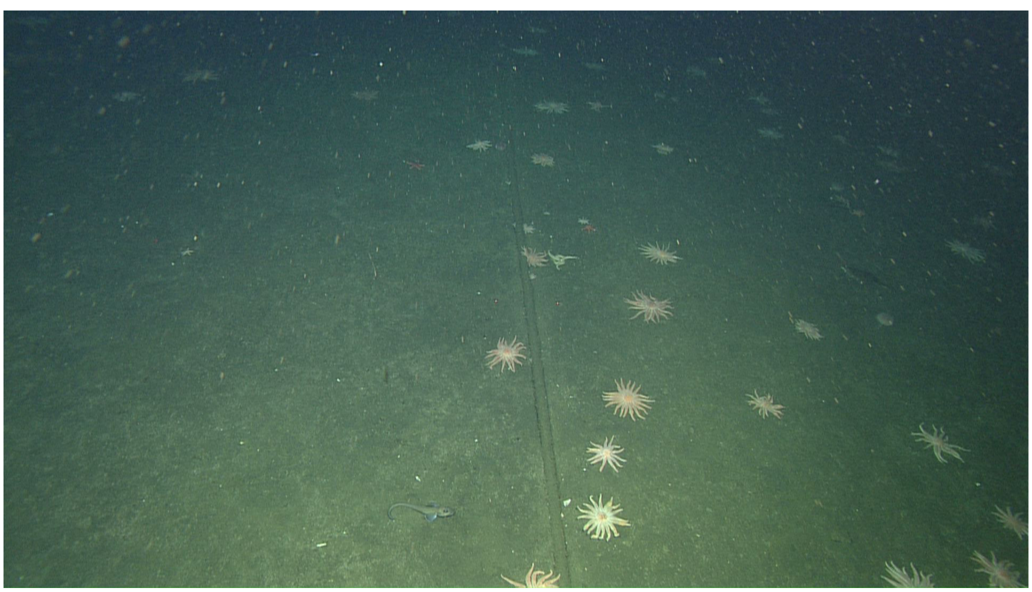

Figure B. In 2007, 79% of the cable was buried along the route. Where the cable is exposed because of underlying hard substrate, 95% of it rested on the seafloor (303 m depth). Settling into surface sediments and mild redistribution over time increased the amount of buried cable to 87.5% with 95% of it resting on seafloor by 2020.

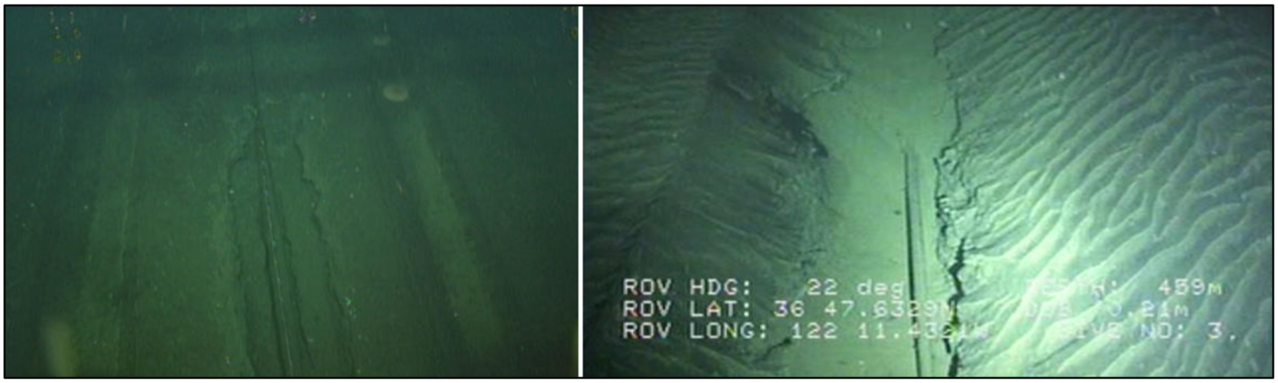

Figure C. At mid-depths, the cable was trenched in and lying below the surrounding sediment surface. The cable was visible within the trench (2007, left = 451 m depth, right = 459 m depth).

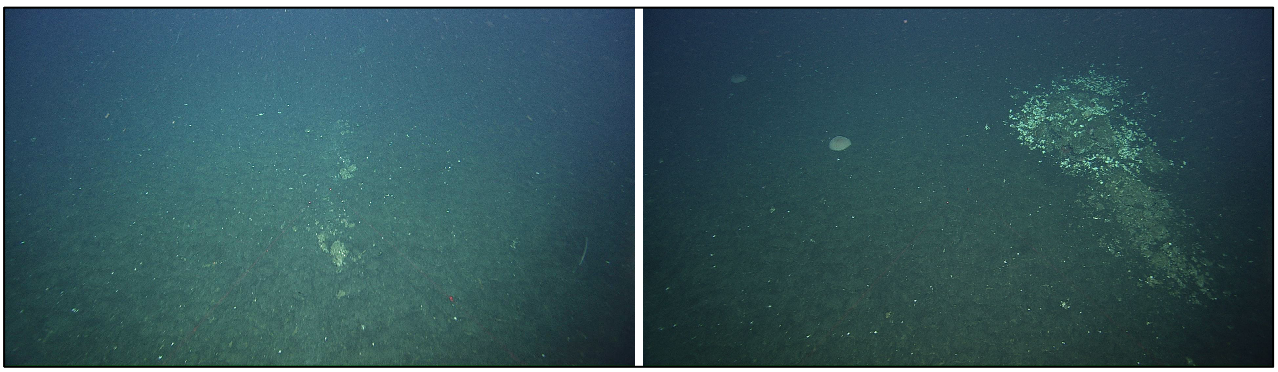

Figure D. These same previously open trenches completed infilled with sediment by about 2010 and only mild disturbance delineates the trench (2020, left = 451 m depth, right = 459 m depth).

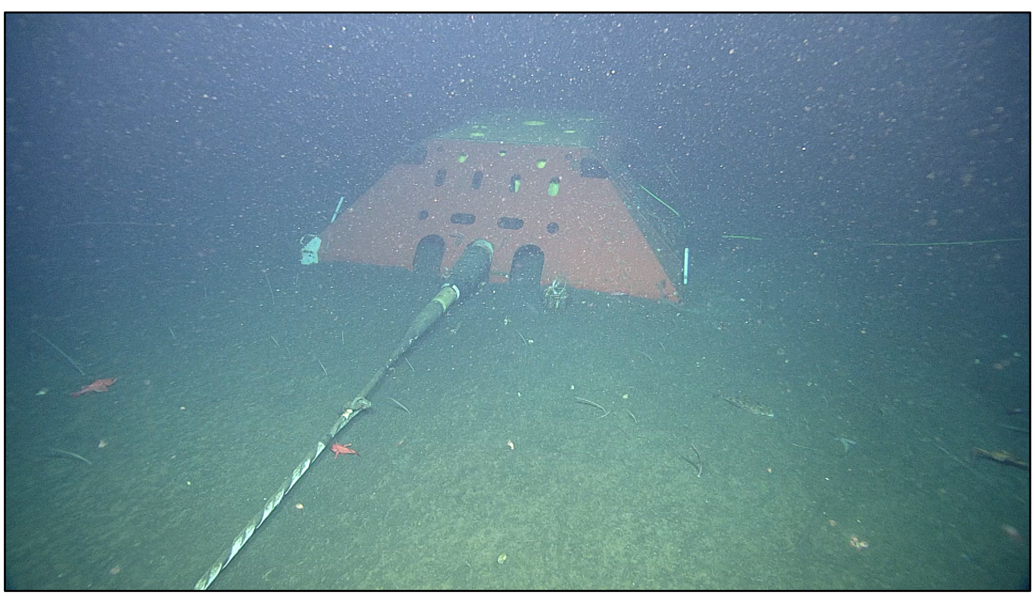

Figure E. The MARS node in 2020 (891 m depth).

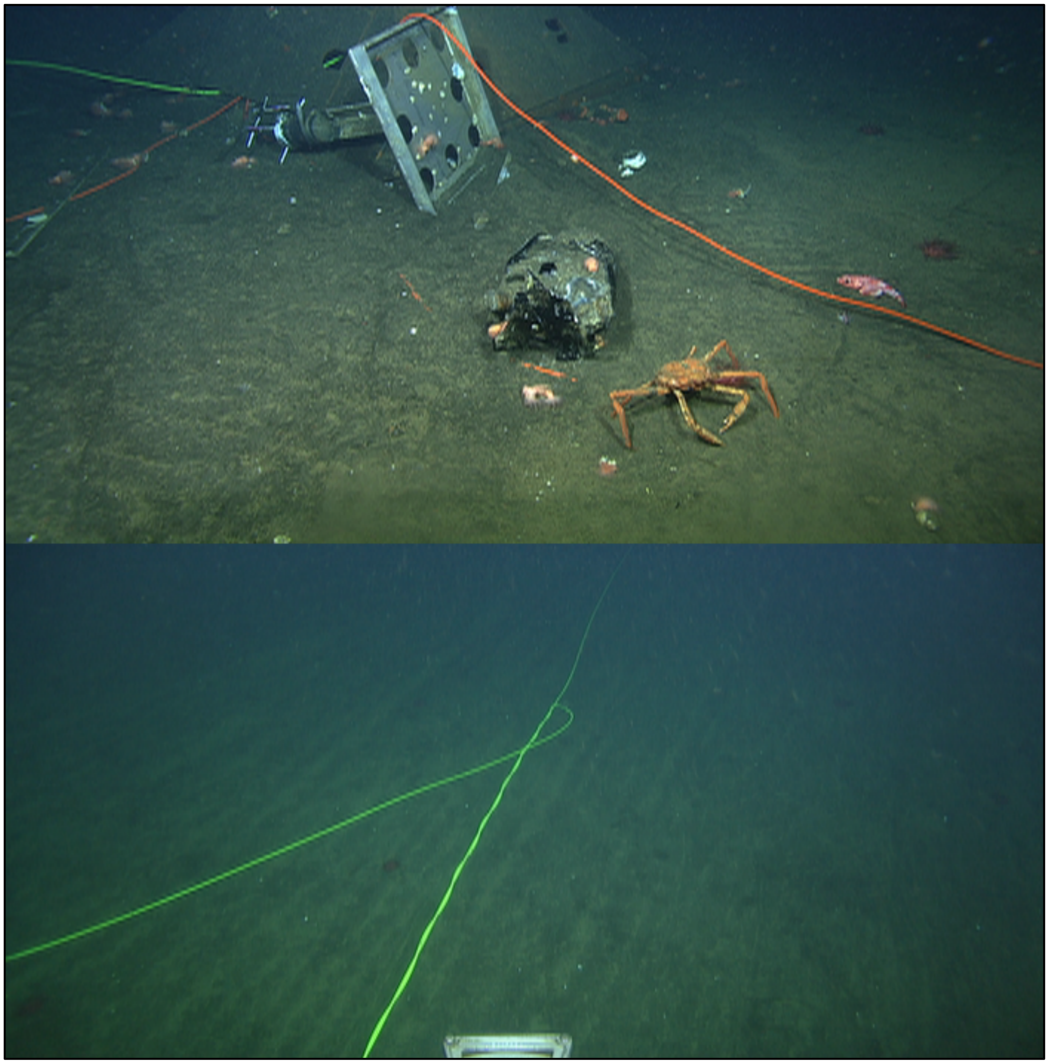

Figure F. Trawl damage near the MARS node with instrument damage. Trawl marks and a displaced auxiliary fiber optic cable.

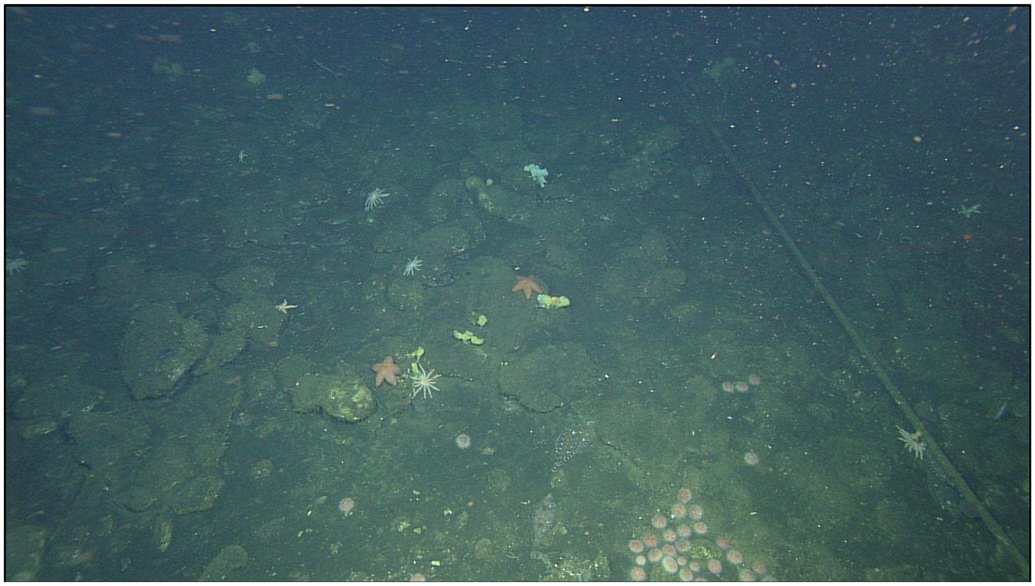

Figure G. The neck of Smooth Ridge is comprised of rocky areas and authigenic carbonate crusts. The MARS cable could not be buried in these areas. The cable is taut here due to small changes in topography (445 m depth).

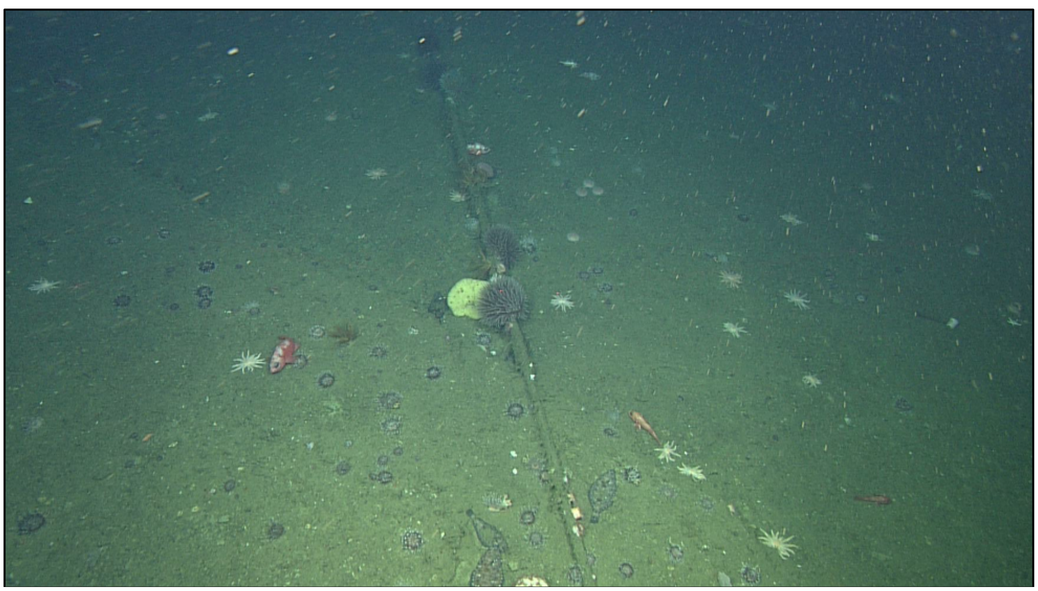

Figure H. Example of a minor point suspension resulting from the presence of a low rock ledge (375 m depth).

Figure I. Typical minor span where rocks or ledges prevent the cable from resting on the seafloor (316 m depth).

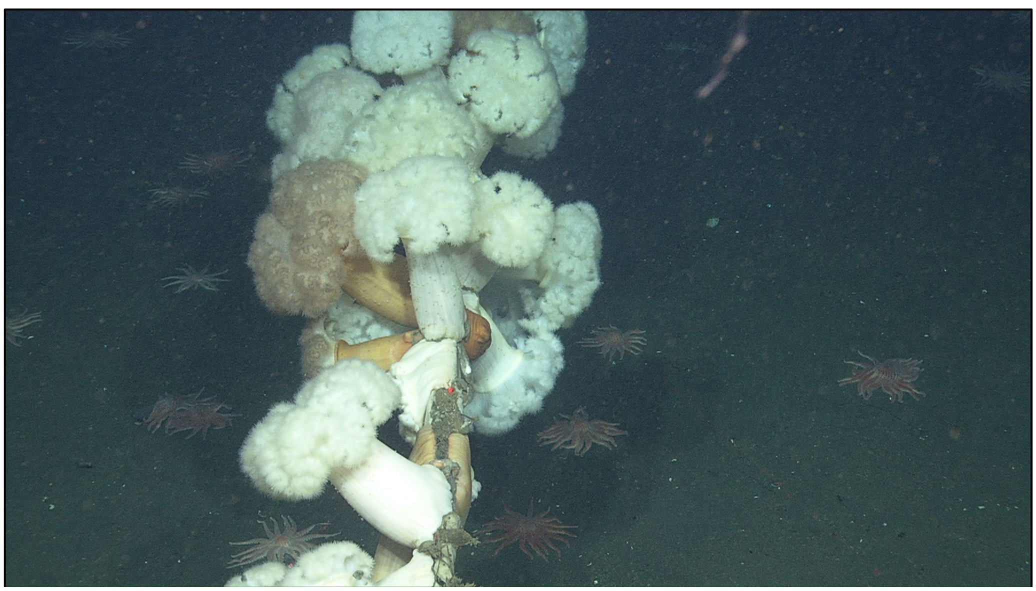

Figure J. Maximum distance the MARS cable is above the seafloor. This span is about 49 m in length and resulted from the presence of rocky ledges on either end of it (191 m depth). This span is around 1.2 m above the seafloor. There is a similar span at 0.5 m high; all others are under 0.2 m high.

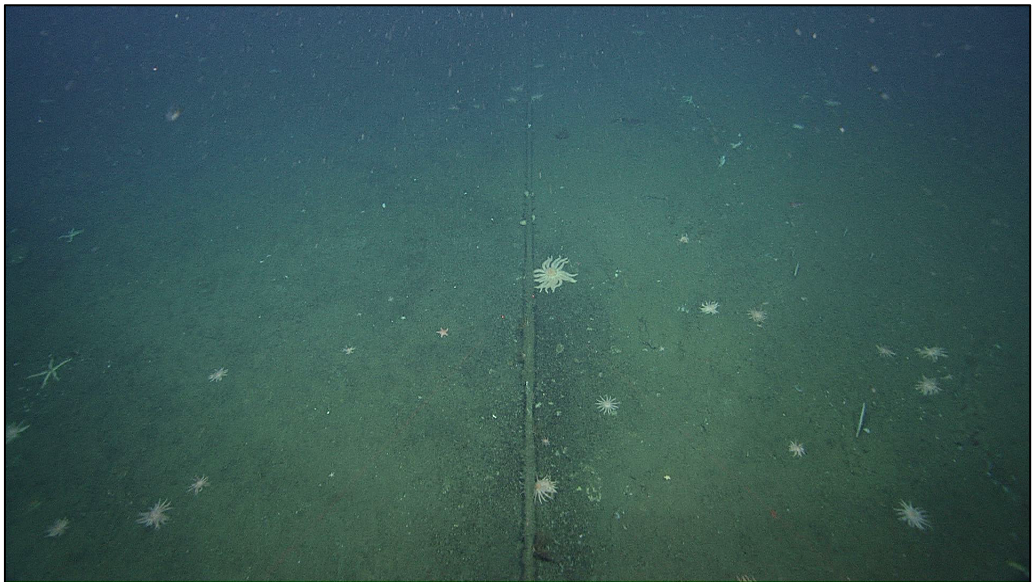

Figure K. Occasional erosion occurred under the cable, resulting from fine sediment winnowing. Larger grainsizes are left behind (350 m).

Figure L. Some areas were draped in deep sediment, with authigenic carbonate underneath. The cable plow brought material to the surface, resulting in large sediment blocks (116 m). Sediment has gradually winnowed away, leaving the authigenic carbonate exposed.

Appendix 3. Mean megafaunal (143 taxa) density on transects along the MARS cable route and control sites (no impact sites were included), with phylum (or subphylum) and group designations. The density (# 100 m^{-2}) of each taxon at regional video transects (n = 168) in all years and at all depths were averaged to produce an overall average density. SE = standard error of the mean. Percent indicates the percentage of the total average faunal density (136 megafaunal individuals 100 m^{-2}).

Phylum	Group	Taxa	Mean Density	SE	%
Cnidaria	Pennatulacea	Funiculina	22.15	3.51	16.3
Echinodermata	Echinoidea	Strongylocentrotus fragilis	13.02	2.17	9.6
Cnidaria	Pennatulacea	Pennatulacea	10.90	1.34	8.0
Cnidaria	Actiniaria	Isosicyonis	10.20	2.19	7.5
Echinodermata	Ophiuroidea	Ophiuroidea	6.62	1.71	4.9
Echinodermata	Asteroidea	Mediaster aequalis	5.78	1.23	4.2
Echinodermata	Holothuroidea	Rathbunaster californicus	5.44	0.84	4.0
Echinodermata	Holothuroidea	Psolus squamatus	5.07	2.13	3.7
Annelida	Polychaeta	Diopatra	4.16	1.75	3.1
Cnidaria	Ceriantharia	Ceriantharia sp. 2	3.98	1.12	2.9
Vertebrata	Pleuronectiformes	Pleuronectiformes	3.55	0.47	2.6
Mollusca	Gastropoda	Gastropoda	3.09	0.65	2.3
Cnidaria	Pennatulacea	Umbellula lindahli	2.89	0.67	2.1
Cnidaria	Actiniaria	Actinostolidae	2.86	0.35	2.1
Arthropoda	Decapoda	Eualus macrophthalmus	2.64	1.32	1.9
Arthropoda	Decapoda	Chionoecetes tanneri	2.52	0.60	1.9
Vertebrata	Sebastidae	Sebastes diploproa	2.31	0.57	1.7
Cnidaria	Ceriantharia	Ceriantharia	1.87	0.23	1.4
Porifera	Porifera	Porifera	1.86	0.38	1.4
Vertebrata	Sebastidae	Sebastolobus	1.37	0.27	1.0
Cnidaria	Actiniaria	Stomphia didemon	1.31	0.20	1.0
Mollusca	Cephalopoda	Octopus rubescens	1.25	0.23	0.9
Vertebrata	Zoarcidae	Lycenchelys crotalinus	1.21	0.22	0.9
Mollusca	Gastropoda	Neptunea-Buccinum Complex	1.06	0.17	0.8
Cnidaria	Actiniaria	Actiniidae sp. 1	1.00	0.18	0.7
Mollusca	Gastropoda	Bathybembix	0.96	0.29	0.7
Vertebrata	Pleuronectiformes	Microstomus pacificus	0.86	0.12	0.6
Cnidaria	Actiniaria	Hormathiidae	0.81	0.20	0.6
Cnidaria	Actiniaria	Urticina	0.79	0.18	0.6
Vertebrata	Pleuronectiformes	Glyptocephalus zachirus	0.77	0.11	0.6
Cnidaria	Pennatulacea	Pennatula phosphorea	0.65	0.22	0.5
Arthropoda	Decapoda	Pagurus tanneri	0.62	0.14	0.5
Vertebrata	Hexagrammidae	Zaniolepis latipinnis	0.55	0.09	0.4
Echinodermata	Holothuroidea	Apostichopus	0.51	0.12	0.4
Vertebrata	Pleuronectiformes	Citharichthys	0.51	0.23	0.4
Echinodermata	Asteroidea	Luidia foliolata	0.48	0.07	0.4
Echinodermata	Asteroidea	Asteroidea	0.45	0.18	0.3
Annelida	Sabellidae	Sabellidae	0.45	0.12	0.3
Vertebrata	Agonidae	Xeneretmus latifrons	0.44	0.08	0.3
Echinodermata	Asteroidea	Crossaster borealis	0.41	0.08	0.3

Phylum	Group	Taxa	Mean Density	SE	%
Echinodermata	Ophiuroidea	Asteronyx longifissus	0.40	0.08	0.3
Vertebrata	Actinopteri	Actinopteri	0.37	0.10	0.3
Cnidaria	Pennatulacea	Virgulariidae	0.31	0.08	0.2
Cnidaria	Actiniaria	Actiniaria	0.30	0.09	0.2
Vertebrata	Stichaeidae	Lumpenus sagitta	0.29	0.11	0.2
Vertebrata	Merlucciidae	Merluccius productus	0.27	0.08	0.2
Cnidaria	Alcyonacea	Heteropolypus ritteri	0.26	0.06	0.2
Mollusca	Gastropoda	Calliostoma	0.25	0.08	0.2
Cnidaria	Pennatulacea	Anthoptilum grandiflorum	0.25	0.11	0.2
Cnidaria	Corallimorpharia	Corallimorphus pilatus	0.25	0.06	0.2
Cnidaria	Actiniaria	Metridium farcimen	0.22	0.05	0.2
Mollusca	Bivalvia	Vesicomyidae	0.21	0.17	0.2
Vertebrata	Myxinidae	Eptatretus	0.19	0.04	0.1
Echinodermata	Asteroidea	Stylasterias forreri	0.19	0.05	0.1
Vertebrata	Pleuronectiformes	Embassichthys bathybius	0.18	0.03	0.1
Cnidaria	Alcyonacea	Swiftia simplex	0.18	0.07	0.1
Vertebrata	Zoarcidae	Lycodes pacificus	0.17	0.05	0.1
Echinodermata	Asteroidea	Halipteris californica	0.16	0.13	0.1
Porifera	Porifera	Cladorhiza	0.16	0.07	0.1
Mollusca	Gastropoda	Pleurobranchaea californica	0.15	0.03	0.1
Echinodermata	Crinoidea	Florometra serratissima	0.15	0.08	0.1
Cnidaria	Ceriantharia	Ceriantharia sp. 1	0.15	0.06	0.1
Arthropoda	Decapoda	Chorilia longipes	0.15	0.03	0.1
Arthropoda	Decapoda	Caridea	0.14	0.10	0.1
Vertebrata	Zoarcidae	Lycodes cortezianus	0.14	0.03	0.1
Vertebrata	Squalidae	Squalus suckleyi	0.12	0.04	0.1
Vertebrata	Pleuronectiformes	Lyopsetta exilis	0.12	0.06	0.1
Vertebrata	Macrouridae	Coryphaenoides	0.12	0.05	0.1
Echinodermata	Asteroidea	Benthopecten	0.11	0.05	0.1
Vertebrata	Zoarcidae	Lycodes diapterus	0.11	0.03	0.1
Vertebrata	Sebastidae	Sebastes saxicola	0.10	0.06	0.1
Vertebrata	Zoarcidae	Lycodapus	0.10	0.04	0.1
Echinodermata	Asteroidea	Hippasteria	0.10	0.02	0.1
Mollusca	Bivalvia	Bivalvia	0.10	0.07	0.1
Cnidaria	Actiniaria	Liponema brevicorne	0.09	0.03	0.1
Vertebrata	Liparidae	Careproctus melanurus	0.09	0.03	0.1
Vertebrata	Rajiformes	Beringaja rhina	0.09	0.03	0.1
Tunicata	Tunicata	Megalodicopia hians	0.08	0.04	0.1
Echiura	Echiura	Echiura	0.08	0.04	0.1
Vertebrata	Sebastidae	Sebastes aurora	0.08	0.03	0.1
Arthropoda	Decapoda	Metacarcinus magister	0.08	0.02	0.1
Vertebrata	Embiotocidae	Zalembius	0.07	0.03	0.1
Cnidaria	Ceriantharia	Ceriantharia sp. 3	0.07	0.03	0.0
Vertebrata	Sebastidae	Sebastes	0.07	0.02	0.0
Echinodermata	Echinoidea	Brisaster	0.06	0.02	0.0
Mollusca	Gastropoda	Gastropoda sp. 3	0.06	0.03	0.0

Phylum	Group	Taxa	Mean Density	SE	%
Vertebrata	Rajiformes	Bathyraja kincaidii	0.05	0.02	0.0
Cnidaria	Pennatulacea	Distichoptilum gracile	0.05	0.02	0.0
Vertebrata	Anoplopomatidae	Anoplopoma fimbria	0.05	0.02	0.0
Mollusca	Cephalopoda	Dosidicus gigas	0.05	0.02	0.0
Vertebrata	Sebastidae	Sebastes semicinctus	0.05	0.03	0.0
Echinodermata	Ophiuroidea	Ophiacanthidae	0.04	0.04	0.0
Vertebrata	Liparidae	Paraliparis cephalus	0.04	0.01	0.0
Mollusca	Gastropoda	Gastropoda sp. 2	0.04	0.02	0.0
Cnidaria	Pennatulacea	Ptilosarcus gurneyi	0.04	0.01	0.0
Annelida	Polychaeta	Serpulidae	0.04	0.03	0.0
Echinodermata	Asteroidea	Asteroidea sp. 1	0.03	0.02	0.0
Vertebrata	Zoarcidae	Bothrocara brunneum	0.03	0.01	0.0
Vertebrata	Moridae	Antimora microlepis	0.03	0.01	0.0
Cnidaria	Rhodaliidae	Dromalia alexandri	0.03	0.01	0.0
Echinodermata	Holothuroidea	Holothuroidea	0.03	0.02	0.0
Arthropoda	Decapoda	Paralithodes	0.03	0.02	0.0
Vertebrata	Sebastidae	Sebastes melanostomus	0.03	0.02	0.0
Mollusca	Gastropoda	Doridacea	0.03	0.01	0.0
Arthropoda	Decapoda	Galatheoidea	0.02	0.02	0.0
Echinodermata	Asteroidea	Henricia sp. 1	0.02	0.02	0.0
Mollusca	Gastropoda	Tritonia tetraquetra	0.02	0.01	0.0
Cnidaria	Alcyonacea	Swiftia kofoidi	0.02	0.02	0.0
Echinodermata	Asteroidea	Goniasteridae	0.02	0.01	0.0
Echinodermata	Asteroidea	Astropecten	0.02	0.01	0.0
Vertebrata	Pleuronectiformes	Parophrys vetulus	0.02	0.01	0.0
Echinodermata	Asteroidea	Myxoderma platyacanthum	0.02	0.01	0.0
Echinodermata	Asteroidea	Poraniopsis	0.02	0.01	0.0
Cnidaria	Anthozoa	Anthozoa	0.02	0.01	0.0
Arthropoda	Decapoda	Decapoda	0.02	0.01	0.0
Arthropoda	Decapoda	Pandalus platyceros	0.02	0.01	0.0
Cnidaria	Alcyonacea	Parastenella	0.02	0.01	0.0
Vertebrata	Torpedinidae	Tetronarce californica	0.01	0.01	0.0
Echinodermata	Ophiuroidea	Asteronyx	0.01	0.01	0.0
Vertebrata	Liparidae	Osteodiscus	0.01	0.01	0.0
Vertebrata	Scyliorhinidae	Parmaturus xaniurus	0.01	0.01	0.0
Vertebrata	Hexagrammidae	Ophidion scrippsae	0.01	0.01	0.0
Arthropoda	Decapoda	Brachyura	0.01	0.01	0.0
Vertebrata	Pleuronectiformes	Eopsetta jordani	0.01	0.01	0.0
Echinodermata	Asteroidea	Henricia sp. 2	0.01	0.01	0.0
Mollusca	Gastropoda	Nudibranchia	0.01	0.01	0.0
Mollusca	Cephalopoda	Octopus californicus	0.01	0.01	0.0
Echinodermata	Holothuroidea	Pannychia mosleyi	0.01	0.01	0.0
Tunicata	Tunicata	Cnemidocarpa finmarkiensis	0.01	0.01	0.0
Vertebrata	Sebastidae	Sebastes jordani	0.01	0.01	0.0
Brachiopoda	Brachiopoda	Laqueus californianus	0.01	0.01	0.0
Arthropoda	Decapoda	Platymera gaudichaudii	0.01	0.01	0.0

Phylum	Group	Taxa	Mean Density	SE	%
Vertebrata	Sebastidae	Sebastes paucispinis	0.01	0.01	0.0
Vertebrata	Pleuronectiformes	Symphurus	0.01	0.01	0.0
Vertebrata	Sebastidae	Sebastes babcocki	0.01	0.01	0.0
Vertebrata	Alepocephalidae	Alepocephalus tenebrosus	0.01	0.00	0.0
Mollusca	Gastropoda	Gastropoda sp. 4	0.01	0.00	0.0
Vertebrata	Chimaeridae	Hydrolagus collei	0.01	0.00	0.0
Vertebrata	Zoarcidae	Lyconema barbatum	0.01	0.00	0.0
Vertebrata	Sebastidae	Sebastomus complex	0.01	0.00	0.0
Vertebrata	Sebastidae	Sebastes elongatus	0.01	0.00	0.0
Mollusca	Cephalopoda	Rossia pacifica	0.01	0.00	0.0
Vertebrata	Rajiformes	Rajiformes	0.01	0.00	0.0
Total			**135.96**	**30.01**	**100.0**